DESIGN AND ANALYSIS OF HEXAGONAL SHAPED FRACTAL ANTENNAS

A THESIS SUBMITTED IN PARTIAL FULFILMENT OF THE
REQUIREMENT FOR THE DEGREE OF

MASTER OF TECHNOLGY
IN
COMMUNICATION AND SIGNAL PROCESSING
BY

SONU AGRAWAL

Roll. No. - 211EC4113

Department of Electronics and Communication Engineering

National Institute of Technology

Rourkela-769 008, India

2013

DESIGN AND ANALYSIS OF HEXAGONAL SHAPED FRACTAL ANTENNAS

A THESIS SUBMITTED IN PARTIAL FULFILMENT OF THE
REQUIREMENT FOR THE DEGREE OF

MASTER OF TECHNOLGY

IN

COMMUNICATION AND SIGNAL PROCESSING

BY

SONU AGRAWAL

Roll. No. - 211EC4113

UNDER THE GUIDANCE OF

Prof. Santanu Kumar Behera

Department of Electronics and Communication Engineering

National Institute of Technology

Rourkela-769 008, India

2013

ACKNOWLEDGEMENT

It is my pleasure and privilege to thank many individuals who made this report possible. First and foremost I offer my sincere gratitude towards my supervisor, **Prof. Santanu Kumar Behera**, who has guided me through this work with his patience. A gentleman personified, in true form and spirit, I consider it to be my good fortune to have been associated with him. I thank **Prof. Sukadev Meher**, Head, Dept. of Electronics & Communication, NIT Rourkela, for his constant support during the whole semester.

I would also like to thank all PhD scholars, especially to **Mr. Ravi Dutt Gupta**, and all colleagues in the microwave laboratory to provide me their regular suggestions and encouragements during the whole work.

Heartily thanks to **Mr. Dayanand Singh**, Scientist/Engineer-'SD', **Mr. Venkata Sitaraman Puram**, Scientist/Engineer-'SC' and **Ms. Sandhya Reddy B**, Scientist/Engineer-'SC', Communication System Group, ISRO Satellite Centre- Bangalore, India for providing measurement facilities in their Laboratory.

Several people have impacted my career positively. I would also like to thank many of my friends, especially **Bijay, Mohit, Suyog, Ankit, Karthik** and **Ravi** for their constant support and inspiration in my quest for higher learning. It is a great pleasure to place on record my gratitude towards all of them.

At last but not the least I am in debt to **My Family** to support me regularly during my hard times.

Sonu Agrawal

Department of Electronics & Communication Engineering
National Institute of Technology Rourkela

CERTIFICATE

This is to certify that the thesis entitled, "**Design and Analysis of Hexagonal Shaped Fractal Antennas***"* submitted by **Mr. Sonu Agrawal** in partial fulfilment of the requirements for the award of Master of Technology Degree in Electronics and Communication Engineering with specialization in **"Communication and Signal Processing"** during session 2011-13 at the National Institute of Technology, Rourkela (Deemed University) is an authentic work carried out by him under my supervision and guidance.

To the best of my knowledge, the matter embodied in the thesis has not been submitted to any other University/Institute for the award of any degree or diploma.

Prof. S K Behera

Contents

ABSTRACT

In this report three antenna designs using fractals have been proposed. Fractal is a concept which is being implemented in microstrip antenna to have better characteristics than conventional microstrip antenna. In the first design, a hexagonal shaped monopole fractal antenna for wideband application is designed. The proposed fractal-like geometry is implemented on a microstrip fed planar hexagonal monopole antenna. The iterated hexagonal fractal patch and modified ground plane are employed to achieve the desired wideband characteristics. A notch is also achieved by introducing slits in ground plane.

In the second proposal, a new hexagonal shaped patch with modified hexagonal carpet ground plane antenna for multiband application is proposed. Its structure is based on carpet fractal geometry introduced in ground plane. The resonance frequency of a conventional hexagonal patch with full ground is lowered by removing carpet of hexagonal elements from the full ground plane. The antenna is optimized for a dual band operation.

The last antenna is the smallest of all the three antennas obtained by taking a hexagonal patch of 8mm side on a fractal ground plane and whole dimension of $30x30mm^2$. Firstly, full ground plane is taken and studied. Then ground plane is modified by introducing and etching out Symmetrical Vertical Pyramidal Structure (SVPS).

All antennas are simulated using CST Microwave Studio Suite 12. For all designs, low cost and readily available FR-4 substrate of relative permittivity of 4.4 and height 1.6mm has been used and fed with 50-ohm microstrip line. All antennas are measured to validate the simulated results. The measured antenna parameters such as return loss, radiation patterns and gain of the proposed antennas are found well matched to the simulated results.

List of Figures

List of Tables

CHAPTER 1

THESIS OVERVIEW

THESIS OVERVIEW

1.1 Introduction

Wireless communication is one of the most blooming areas in the communication field today. It means the transfer of information between two or more points that are not connected by an electrical conductor. Wireless operations allow facilities, such as distant communications, that are tough or impractical to implement with the use of wires and it is costly too. In numerous homes and offices, the mobile phones free us from the short leash of handheld cords. Cell phones give us even more freedom such that we can communicate with each other at any time and in any place. Wireless local area network (WLAN) technology provides us access to the internet without suffering from managing yards of unsightly and expensive cable. Information is transferred over both short and long distances. These wireless phones use radio waves to enable their users to make phone calls from many locations worldwide.

Since 1960s, it has been a topic of study but the past decade has seen a downpour of research activities in the area. This is due to a union of several factors. To start with, an explosive increase in demand for tetherless connectivity is one of the major factors which are driven so far mainly by cellular telephony. Second, the dramatic progress in VLSI technology has enabled small-area and low-power implementation of sophisticated signal processing algorithms and coding techniques. Also the need of compact and handy communication systems is also one of prime reason behind this.

The maximum achievable data rate or capacity for the ideal band-limited additive white Gaussian noise (AWGN) channel is related to the bandwidth and signal-to-noise ratio (SNR) by Shannon-Nyquist criterion [1, 2], as shown in Eq. 1.1.

$$C = B \log_2 (1 + SNR) \tag{1.1}$$

where *C* denotes the channel capacity, *B* stands for the channel bandwidth.

Eq. 1.1 indicates that the total channel capacity can be increased by increasing the bandwidth occupied by the signal or by increasing the transmission power of the signal. However, the transmission power cannot be readily increased because many portable devices are battery powered and the potential interference should also be avoided. Thus, to achieve high data rate, a wide frequency bandwidth will be the only solution.

In 2002, Federal Communication Commission (FCC) allocated the bandwidth 3.l-10.6GHz for commercial use and named it as UWB frequency band. The frequency band of operation is based on the –10dB bandwidth of the UWB emission. Wireless communications permits UWB technology to overlay already available services such as the Wi-MAX and the IEEE 802.11 WLANs that coexist in the 3.1 to 10.6GHz. According to the FCC's rule, any signal that occupies at least 500MHz spectrum or whose fractional bandwidth is greater than 0.25 can be used in UWB systems. It means that UWB is not restricted to impulse radio any more. It is also applicable to all the technology that uses 500MHz spectrum and complies with all other requirements for UWB [3]. The fractional bandwidth *'B'* is given by the formula

$$B = \frac{f_2 - f_1}{f_c} \tag{1.2}$$

where, f_2 and f_1 are upper and lower edge frequencies respectively whereas f_c is central frequency.

UWB technology offers noteworthy benefits for consumers, public safety, and Government aided services. It is believed that the greatest potential use of UWB is in short-range communications in the home or business, allowing equipment mobility and high data rates to facilitate information sharing. UWB radio will supply the essential new wireless bandwidth cheaply, without using any precious and limited radio frequencies. So it has a

significant role to play as an extension or complement to cellular technology in future mobile systems.

These days, demand of seamless integration of cellular networks such as GSM & 3G and WLAN & WPAN is increasing which is a strong indicator for the inclusion of high-speed short range wireless in a broad picture of future wireless networks. The rapid development of Wireless communication system is bringing about a wave of new wireless devices and systems to meet the demands of multimedia applications. Cellular phones, wireless local area networks (WLANs) and wireless personal area networks (WPANs) place several demands on the small and multi-purpose antennas. Primarily, the antennas need to small dimension, high gain, wide bandwidth, embedded installation, etc. In particular, the impedance bandwidths, polarization or axial ratio, radiation patterns and gain are becoming the most important factors that affect the application of antennas in contemporary and future wireless communication systems [4].

Table 1.1 shows the operating frequencies of some of the most commonly used wireless communication systems. The bandwidths vary from 7% to 13% for commercial mobile communication systems, and reach up to 109% for ultra-wideband communications. The antennas used must have the required performance over the relevant operating frequency range. Antennas for fixed applications such as cellular base-stations and wireless access points should have high gain and stable radiation coverage over the operating range. Antennas for portable devices such as headphones, personal digital assistants (PDAs) and laptop computers should be embedded, efficient in radiation and omnidirectional in coverage. Most importantly, the antennas should be well impedance-matched over the operating frequency range [4].

Table 1.1 Wireless communication system frequencies.

System	Operating frequency	Overall bandwidth
Advanced Mobile Phone Service (AMPS)	Tx: 824–849MHz Rx: 869–894MHz	70 MHz (8.1 %)
Global System for Mobile Communications (GSM)	Tx: 880–915MHz Rx: 925–960MHz	80MHz (8.7 %)
Personal Communications Service (PCS)	Tx: 1710–1785MHz Rx: 1805–1880MHz	170MHz (9.5 %)
Global System for Mobile Communications (GSM)	Tx: 1850–1910MHz Rx: 1930–1990MHz	140MHz (7.3 %)
Wideband Code Division Multiple Access (WCDMA)	Tx: 1920–1980MHz Rx: 2110–2170MHz	250MHz (12.2 %)
Universal Mobile Telecommunication Systems (UMTS)	Tx: 1920–1980MHz Rx: 2110–2170MHz	250MHz (10.2 %)
Ultra-wideband (UWB) communications and measurement	3100–10 600MHz	7500MHz (109 %)

1.2 Thesis Motivation

In recent years, modern telecommunication systems require antennas with wider bandwidth and smaller dimension rather than conventional ones. Most importantly, the antennas should be well impedance-matched over the operating frequency range. Narrowband operation of antennas has become a necessity for many applications too. In recent wireless communication systems, dual band as well as single band behaviour with good gain is the need for many applications, such as GPS, GSM services operates at two different frequency bands. WLAN, Wi-Fi systems require single band operation. In this wireless world, integration of many applications is also required. So it requires same antenna to work for all of the integrated applications.

Design of conventional microstrip patch with bandwidths as low as a few per cents, wideband applications are very limited. Other disadvantages include low gain, low power handling capability, high Q value and poor polarization purity. For over two decades, researchers have proposed several methods to achieve miniaturization, improvement in bandwidth in case of wideband behaviour and realizing narrowband characteristics using planar microstrip antenna. Due to unique advantages such as small volume, low manufacturing cost and easy integration into planar circuits, planar microstrip antennas are ideal candidates.

Another method to have compact and small volume antenna is by using fractals in the planar microstrip antenna geometry. Fractalisation of planar antenna will help in make antenna more efficient. It will expand the bandwidth and reduce the dimensions of the antenna [5]. Fractals will increase the total electrical length of the antenna keeping the total area same. It helps in miniaturization of antenna. Size can be shrunk from two to four times with surprising good performance. Multiband performance can be achieved at non-harmonic frequencies.

1.3 Literature Review and Methodology

The invention of Microstrip patch antennas has been attributed to several authors, but it was certainly dates in the 1960s with the first works published by Deschamps, Greig and Engleman, and Lewin, among others. Since 1970, rigorous research publications came into picture with the first design equations. Since then different authors started investigations on Microstrip patch antennas like James Hall and David M. Pozar and many more who contributed a lot. In high performance aircraft, spacecraft, satellite and missile applications, where size, weight, cost, performance and ease of integration, low profile antenna are required. To meet these requirements microstrip antenna can be used. The antennas discussed earlier are 3-dimensional antennas which are bulky and need more space to be deployed. MSA are the modern generation of antennas, having attractive features such as light weight, low cost, small in size and ease of integration into arrays. These boastful features make them ideal components of modern communications systems, particularly in cellular and WLAN applications.

The main purpose of this thesis is to design antennas using fractal technique on microstrip antenna to achieve miniaturization, thereby, achieving wideband as well as narrowband characteristics using hexagonal structure. Different fractal techniques are employed to get both the behaviour. Hexagonal gasket is used with partial ground plane to achieve wideband behaviour whereas narrowband characteristics is realised by doing employing fractal technique to modify full ground plane keeping same hexagonal patch of smaller dimension.

Of all the quadrilaterals, hexagon forms the most compact geometry having area coverage more than other basic shapes like circle and triangle. That is why shape of cell is hexagonal in cellular network. By taking simple hexagonal patch itself will show good behaviour. But to get desired characteristics with reduced dimension, some technique must be

employed. Therefore it is taken as a base structure for all the designs to realize all the behaviour.

The term "fractal" was first used by mathematician Benoit Mandelbrot in 1975. Rumsey, a well-known scientist, established that an antenna with shapes only defined by angles would be frequency independent, since it would not have any characteristics size to be scaled with wavelength. He was sometimes referred to as the father of fractal geometry, who said, “I coined fractal from the Latin adjective *fractus*”. The word fractal is derived from the Latin word “fractus” meaning broken, uneven, any of various extremely irregular curves or shape that repeat themselves at any scale on which they are examined. Using fractal in an antenna maximizes the length, or increase the perimeter (on any side of structure), of material that can receive or transmit electromagnetic radiation within a given total surface area or volume. There are different types of fractals which reveal that as you zoom in on the image at finer and finer scales, the same pattern re-appears so that it is virtually impossible to know at which level you are looking.

Fractal is a concept which is being implemented in microstrip antenna to have better characteristics than microstrip antenna. In many fractal antennas, the self-similarity and plane-filling nature of fractal geometries are often quantitatively linked to its frequency characteristics. Fractals are self-similar geometrical shapes which repeat themselves at different scales. The geometry of fractals is important because the effective length of the fractal antennas can be increased while keeping the total area same.

1.4 Thesis Outline

The outline of this thesis is as follows.

Chapter 2: This chapter presents the basic theory of MSAs, including the basic microstrip patch geometries, features, different feeding methods describing their characteristics, the

advantages and disadvantages of MSAs. Finally different calculations are shown to calculate the feedline width and other dimensions of MSA. This chapter ends with the introductory part of the numerical method, Finite Element Method (FEM), which is helpful to analyse any complex geometry.

Chapter 3: This chapter deals about fractal geometry. Fractal antenna engineering represents a relatively new field of research that combines attributes of fractal geometry with antenna theory. Chapter presents basic theory of fractals describing its features, classes, and dimensions and explained about Iterative function schemes (IFS). The performance of the fractal antenna with respect to conventional Euclidean geometry has also been discussed. The chapter ends by describing the advantages and disadvantages of using fractals in microstrip antenna.

Chapter 4: This chapter describes the design of wideband antenna using CST Microwave Studio Suite 12. The simulated and measured results are presented in terms of different antenna parameters such as return loss, gain, radiation patterns measurements. The effect of slots and slits in the partial ground plane are shown. Different parametric studies have also been shown.

Chapter 5: In this chapter the narrowband antenna designs are described. The effect of different ground planes is discussed. The different properties of antennas are studied and simulated using CST Microwave Studio Suite 12. Finally comparison between the simulation and theoretical results are presented..

Chapter 6: This chapter contains conclusion and scope of future work

CHAPTER 2

MICROSTRIP ANTENNA

MICROSTRIP ANTENNA

This chapter deals with the microstrip antennas which are small in size and much lighter than the antennas discussed in the previous chapter. Though, the antennas already discussed are also used, but planar antennas have their own advantages which will be discussed here. The basic geometries, feeding techniques, features and applications of planar antennas are illustrated here.

2.1 Microstrip Antenna (MSA)

The idea of microstrip antenna was traced in 1953 [6] and a patent in 1955 [7]. But it received considerable attention in the start of 1970s. In high performance aircraft, spacecraft, satellite and missile applications, where size, weight, cost, performance and ease of integration, low profile antenna are required. To meet these requirements microstrip antenna can be used [8]. The antennas discussed earlier are 3-dimensional antennas which are bulky and need more space to be deployed. MSA are the modern generation of antennas having attractive features as low profile, low cost, light weight and ease of integration into arrays. These features make them ideal components of modern cellular and WLAN applications [9].

With increasing requirements for personal and hand-held mobile communications, the demand for compact and low-cost antennas has brought the MSA to the forefront. A MSA in its simplest form consists of a radiating patch on front side of a dielectric substrate and a ground plane on the back side. The top and side views of a rectangular MSA (RMSA) are shown in Fig. 2.1. Often microstrip antennas are also referred to as *patch* antennas. The radiating elements and feed lines are usually photoetched on the dilelectric substrate. The radiating patch may be square, circular, triangular, semi-circular, sectoral, and annular ring shapes shown in Fig. 2.2.

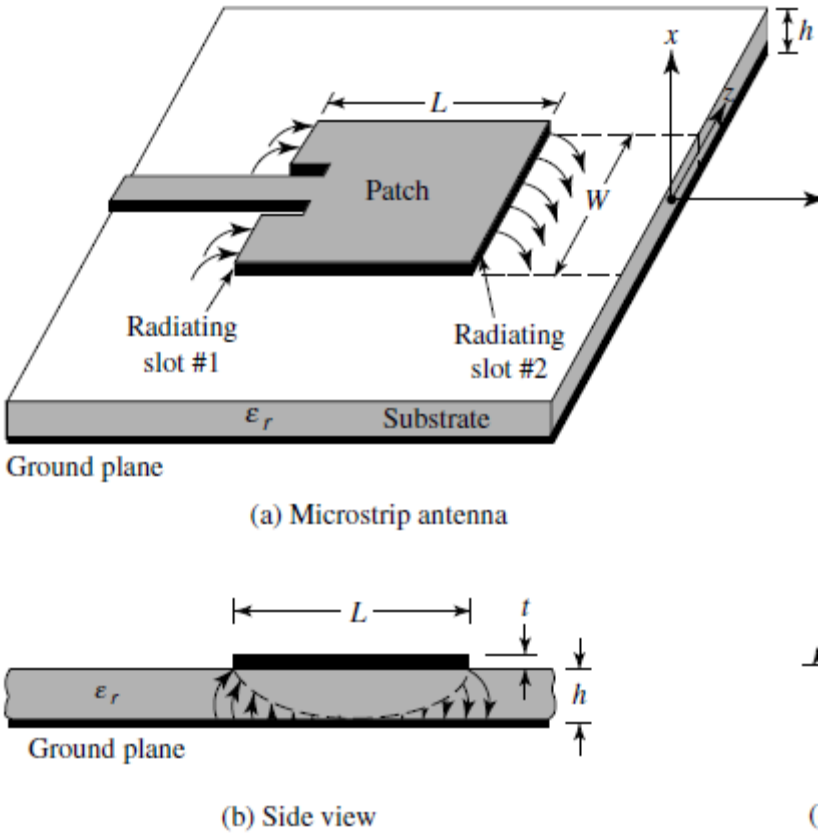

Figure 2.1 MSA configurations with its side view

Also evaluation of the basic properties of microstrip patch antennas (MPA) has been numerously discussed in literature [10], [11].

There are basically two types of radiator. One is broadside and other is end-fire radiator. Broadside radiators are those whose maximum pattern is normal to the patch or axis of the antenna whereas end-fire radiators are those whose maximum is along the axis of the antenna. The microstrip patch is designed so that its pattern maximum is normal to the patch i.e. it is generally behaves as broadside radiator. This is accomplished by properly choosing the mode i.e. field configuration of the excitation beneath the patch. End-fire radiation can also be possible by judicious mode selection. The strip and ground plane are separated by a dielectric sheet as shown in Fig. 2.1.

There are several substrates that can be used for the design of microstrip antennas. The dielectric constants are usually in the range of $2.2 \leq \varepsilon_r \leq 12$. Most desirable for good

antenna performance is thick substrates whose dielectric constant is low because they provide better efficiency, larger bandwidth, loosely bound fields for radiation into space, but it will cost us in larger element size. Thin substrates with higher dielectric constants are also

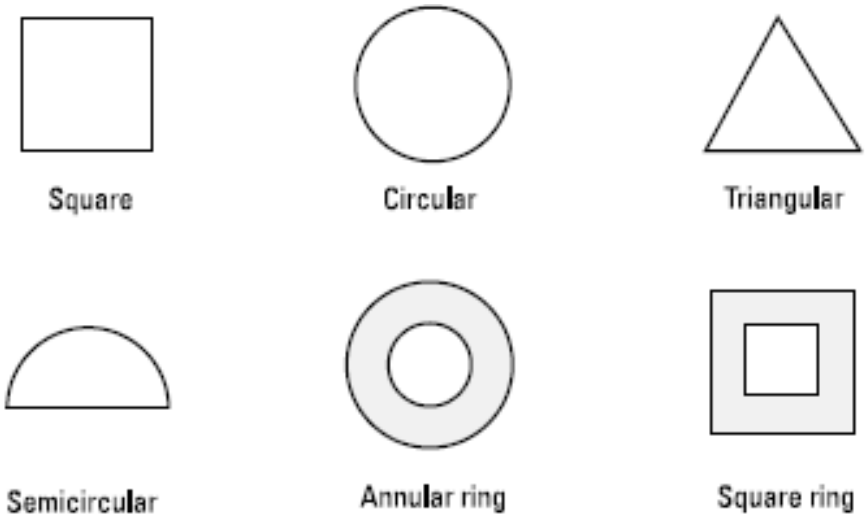

Figure 2.2 Different shapes of microstrip patches

used for the microwave circuitry as they require tightly bound fields to minimize undesired radiation and coupling which lead to smaller element sizes. However, they are less efficient and have relatively smaller bandwidths on account of greater losses [12].

Since microstrip antennas are often integrated with other microwave circuitry, a compromise has to be reached between good antenna performance and circuit design [8].

2.1.1 Feeding Methods

There are different feeding methods employed to feed the microstrip antennas. The most popular techniques are microstrip line, coaxial probe, aperture coupling and proximity coupling [8].

The microstrip feed line is also called conducting strip, generally of much smaller width compared to the patch. The microstrip line feed is easy to fabricate and simple to match

by controlling the inset position and rather simple to model. However as the substrate thickness increases surface waves and spurious feed radiation increase, which for practical

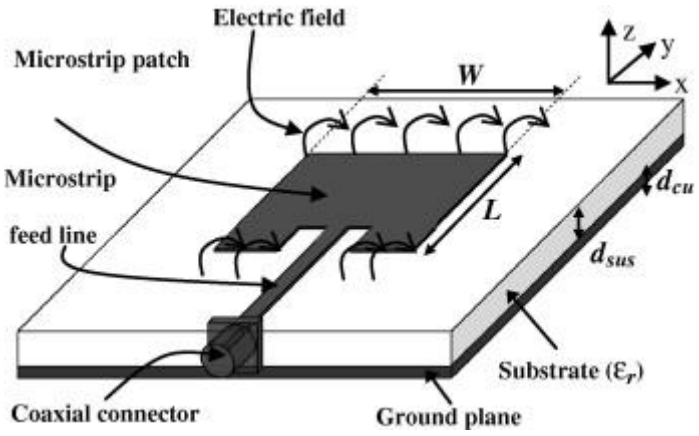

Figure 2.3 Microstrip line feed

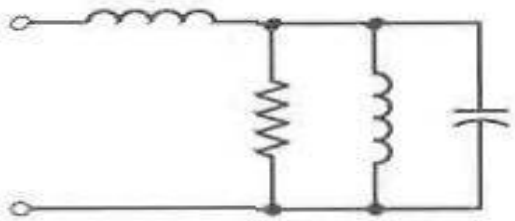

Figure 2.4 Equivalent circuit of microstrip feed line

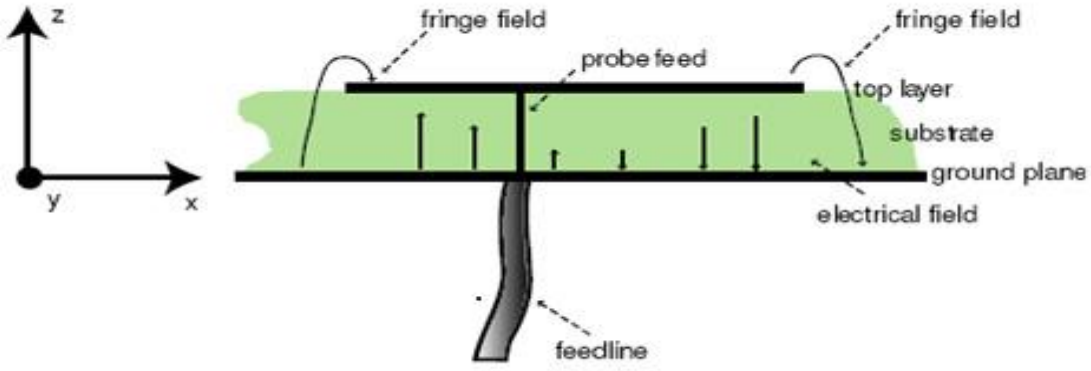

Figure 2.5 Coaxial line feed

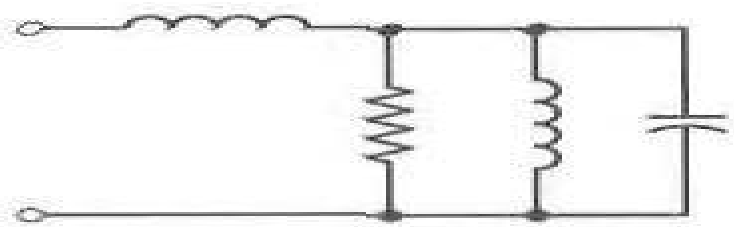

Figure 2.6 Equivalent circuit of coax feed line

designs limit the bandwidth (typically 2-5%). A typical microstrip feed line and its equivalent circuit are shown in Figs. 2.3 and 2.4, respectively.

Coaxial-line feeds, where the inner conductor of the coax is attached to the radiation patch while the outer conductor is connected to the ground plane, are also widely used. The coaxial probe feed is also easy to fabricate and match, and it has low spurious radiation. However, it also has narrow bandwidth and it is more difficult to model, especially for thick substrates. A typical coax feed and its equivalent circuit are also shown in Figs. 2.5 and 2.6, respectively, where inner conductor is attached to the patch and outer to the ground plane.

Both the microstrip line and probe possess inherent asymmetries which generate higher order modes which produce cross-polarized radiation. To overcome some of the problems, non-contacting aperture coupling feeds have been introduced. The aperture coupling is most difficult to fabricate. However, it is somewhat easier to model and has moderate spurious radiation.

As shown in Fig. 2.7, aperture coupling consists of two substrates separated by a ground plane. On the bottom side of the lower substrate, there is a microstrip feed line whose energy is coupled to patch through a slot on the ground plane separating the two substrates. Its equivalent circuit is described by Fig. 2.8. This arrangement allows independent optimization of the feed mechanism and the radiating element. Typically a high dielectric material is used for the bottom substrate, and thick low dielectric constant material for the top

substrate. The ground plane between the substrates also isolates the feed from the radiating element and minimizes interferences of the spurious radiation for pattern formation and polarization purity. For this design, the substrate electrical parameters, feed line width, and slot size and position can be used to optimize the design. Typically matching is performed by controlling the width of the feed and the length of the slot.

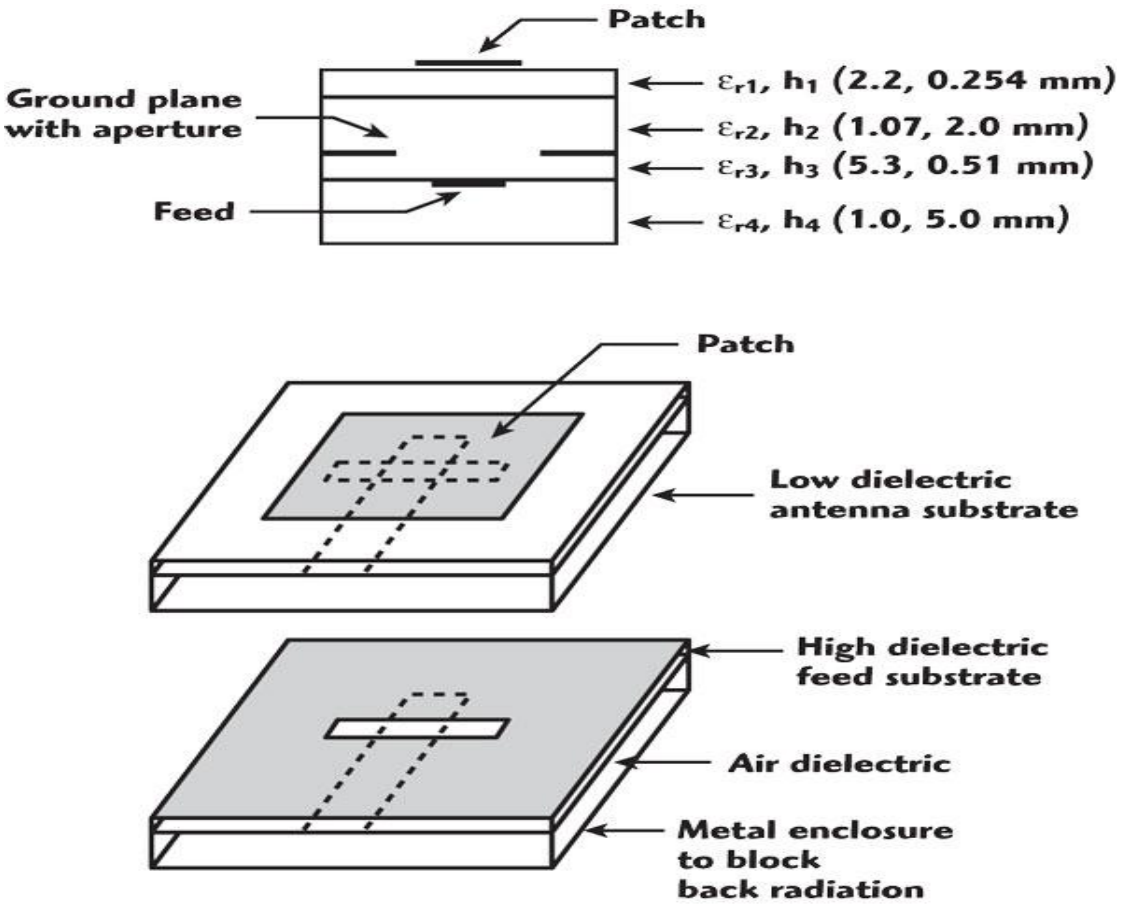

Figure 2.7 Aperture coupled feed

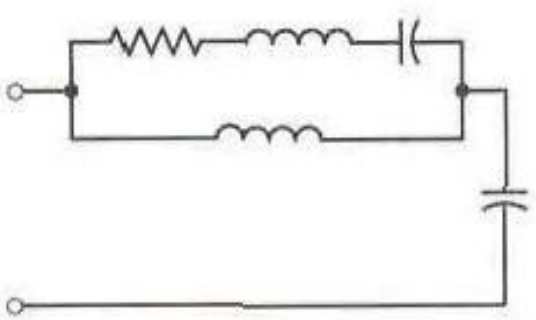

Figure 2.8 Equivalent circuit of aperture coupled feed

The most severe demerit of microstrip antennas is their small bandwidth. As microstrip antennas are having small bandwidth, so there is need to have some mechanism to increase its bandwidth. One of the most advantageous methods is by proximity coupling. There are basically two types of bandwidths, one is *impedance bandwidth* (the bandwidth over which the antenna remains matched to the feedline to some specified level, such as (VSWR $\leq$ 2), and the *pattern bandwidth* (the bandwidth over which the pattern remains, in some sense, constant). The ideal broadband element will satisfy both the criteria.

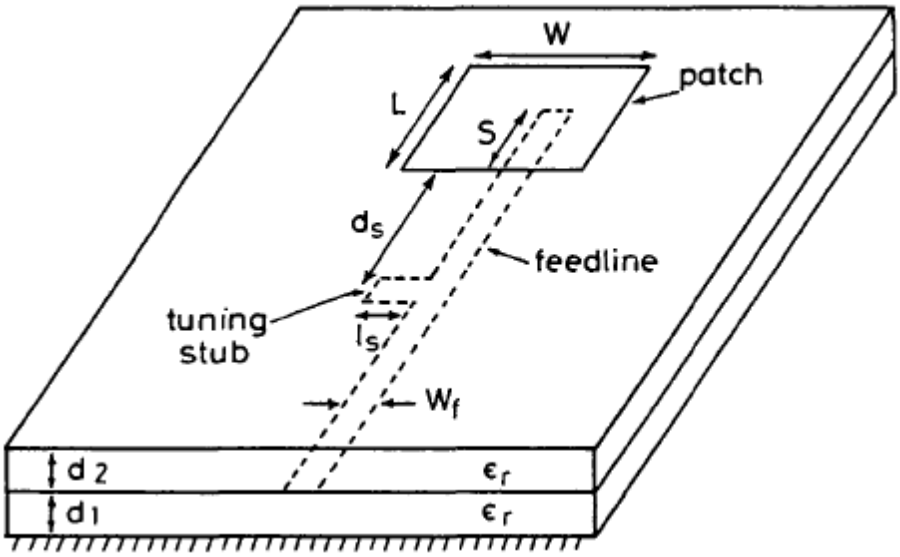

Figure 2.9 Proximity coupled feed

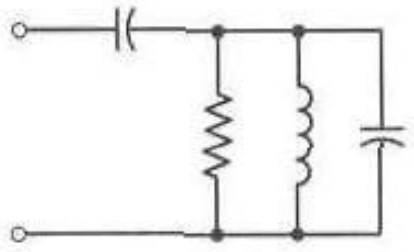

Figure 2.10 Equivalent circuit of proximity coupled feed

The enhanced bandwidth is obtained by using a microstrip feed line proximity-coupled to a patch antenna printed on a substrate above the feedline as shown in Fig.2.9 [13]. Its equivalent circuit is shown in Fig.2.10.

2.1.2 Structural Analysis of MSA

There are different models of MSA. The simplest of all the models is transmission line model. It is easiest but the disadvantage of using it is it yields less accurate results and it lacks the versatility. Basically the transmission line model represents the microstrip antenna by two slots separated by a low-impedance Z_c transmission line of length L, width W and height H, as shown in Fig.2.11.

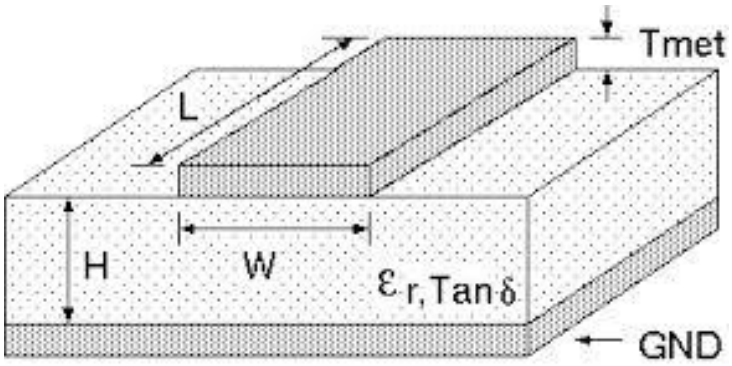

Figure 2.11 Microstrip line

2.1.2.1 Fringing Effects

As the dimensions of the patch are finite along the length and width, the fields at the edges of the patch undergo fringing. This is illustrated in Fig.3.12 for the two radiating slots of the microstrip antenna. The amount of fringing is a function of the dimensions of the patch and the height of substrate. For a microstrip line, typical electric field lines are shown in Fig.2.12. This is a nonhomogenous line of two dielectrics; typically the substrate and air. As it can be seen from the figure, most of the electric field lines reside in the substrate and parts of some lines exist in air. As W/H $\gg$ 1 and $\in_r \gg 1$, the electric field lines concentrate mostly on the

substrate. Fringing in this case makes the microstrip line look wider electrically compared to its physical dimensions. Since some of the waves travel in the substrate and some in air, an *effective dielectric constant (EDC)* $\in_{reff}$ is introduced to account for fringing and the wave propagation in the line [8].

For most applications, where the dielectric constant of the substrate is much greater than unity ($\in_r \gg 1$), the value of $\in_{reff}$ will be closer to the value of the actual dielectric constant $\in_r$ of the substrate. For a line with air above the substrate, the EDC has the values in the range of $1 < \in_{reff} < \in_r$. EDC depends on frequency of operation too. As the operating frequency increases, most of the electric field lines concentrate in the substrate [8].

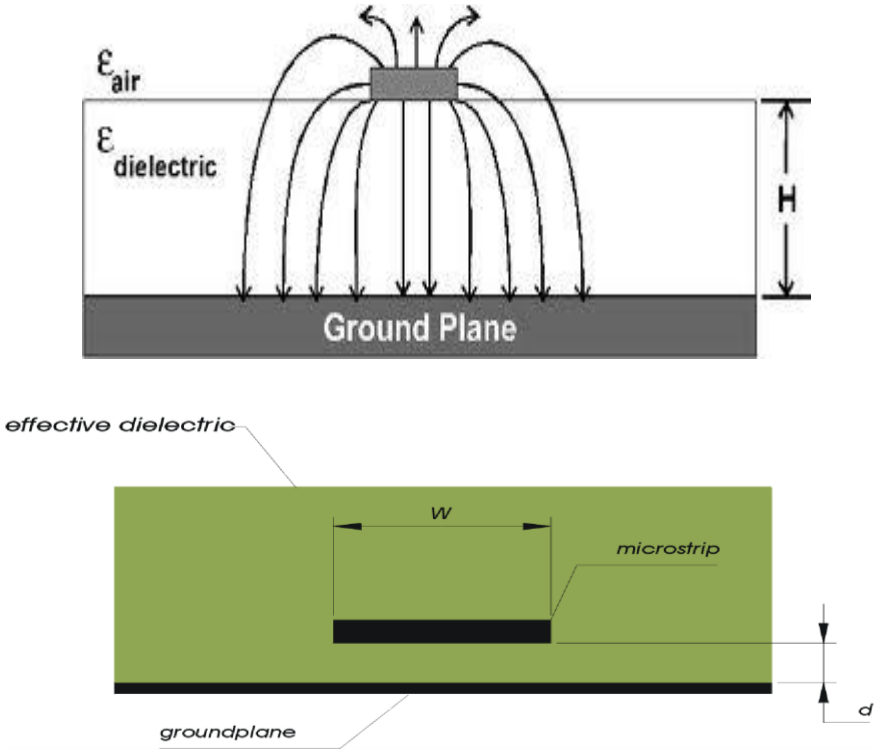

Figure 2.12 Microstrip E-field lines and its effective dielectric constant

For low frequencies, EDC is nearly constant. At the intermediate frequencies its values begin to increase slowly and ultimately approach the values of the dielectric constant of the substrate. The initial or static value at low frequency of EDC is given by Eq. 2.1. This value is valid for W/H > 1.

$$\epsilon_{reff} = \frac{\epsilon_r+1}{2} + \frac{\epsilon_r-1}{2}\left(\frac{1}{\sqrt{1+\frac{12H}{W}}}\right) \quad (2.1)$$

where W is width of feedline and 'H' is weight of the substrate.

The characteristics impedance Z_o of the microstrip feed line also depends on the width W of the feedline and height H of the substrate and it is having different values for W/H ≤ 1 and W/H ≥ 1 as illustrated in the Eqs.2.2 and 2.3.

$$Z_o = \frac{60}{\sqrt{\epsilon_{reff}}}\ln\left(\frac{8H}{W} + \frac{W}{4H}\right); \qquad \frac{W}{H} \leq 1 \quad (2.2)$$

$$= \frac{120\pi}{\sqrt{\epsilon_{reff}}} ln\left(\frac{8H}{W} + \frac{W}{4H}\right); \qquad \frac{W}{H} \geq 1 \quad (2.3)$$

The width W of the line and height H of the substrate is decided by parameters A and B which are dependent on the characterictics impedance of the line and dielectric constant of the substrate as shown in Eqs.2.4, 2.5, 2.6 and 2.7.

$$\frac{W}{H} = \frac{8e^A}{e^{2A}-2}; \qquad \frac{W}{H} < 2 \quad (2.4)$$

$$\frac{W}{H} = \frac{2}{\Pi}\left[B - 1 - \ln(2B-1) + \frac{\epsilon_r-1}{2\epsilon_r}\left\{\ln(B-1) + 0.39 - \frac{0.61}{\epsilon_r}\right\}\right];$$

$$\frac{W}{H} > 2 \quad (2.5)$$

where

$$A = \frac{Z_o}{60}\sqrt{\frac{\epsilon_r+1}{2}} + \frac{\epsilon_r-1}{\epsilon_r+1}\left(0.23 + \frac{0.11}{\epsilon_r}\right); \quad (2.6)$$

and $$B = \frac{377\Pi}{2\,Z_o\sqrt{\epsilon_r}}; \quad (2.7)$$

For the principal E-plane (xy-plane), fringing is a function of the ratio of the length of the patch L to the height H of the substrate (L/H) and dielectric constant $\in_r$ of the substrate. For microstrip antenna, $\frac{L}{H} \gg 1$, so fringing is very less. But fringing must be reduced and taken into account because it influences the resonant frequency of the antenna.

Generally, the characteristics impedance of the feedline is taken as 50Ω. The reason behind choosing this are described below:

- Practically, all available source ports are having 50Ω internal impedance. So by *Maximum Power Theorem*, we have to select 50Ω as the characteristics impedance for the feedline of the microstrip antenna to transfer maximum power from source to load.
- Theoretically, it has been found that 76Ω is required for minimum attenuation in the line and 37Ω is needed for maximum power transfer from the line. So to compromise between these two, we are selecting the average of the above two values and by rounding off the average value, we will get 50Ω as the characteristics impedance for the feedline.

2.1.3 Advantages and Disadvantages of MSA

Microstrip Patch antennas are widely used in today's era. It is used in satellite communication, military purposes, GPS, mobile, missile systems etc. Bearing in mind the features of microstrip antenna, there are many advantages and disadvantages as well. Some of them are discussed below.

2.1.3.1 Advantages

MSAs have several advantages compared to the conventional microwave antennas. The main advantages of MSAs are listed as follows:

- They are lightweight and have a small volume and a low-profile planar configuration.
- They can be made conformal to the host surface.
- Their ease of mass production using printed-circuit technology leads to a low fabrication cost.
- They are easier to integrate with other MICs on the same substrate.
- They allow both linear polarization and circular polarization.
- They can be made compact for use in personal mobile communication.
- They allow for multi-frequency operations.

2.1.3.2 Disadvantages

MSAs suffer from some disadvantages as compared to conventional microwave antennas. They are illustrated as follows:

- They have narrow impedance bandwidth.
- They are having low gain.
- Extra radiation occurs from its feeds and junctions
- Low power-handling capability
- Their efficiency is very less.
- Poor-polarization purity
- High Q value

The quality factor is a figure-of-merit that is representative of the antenna losses. There are different types of losses such as radiation, conduction, dielectric and surface wave losses. The total quality factor Q_t is influenced by all of these losses [14] and is, in general, given by Eq. 2.8.

$$\frac{1}{Q_t} = \frac{1}{Q_{rad}} + \frac{1}{Q_c} + \frac{1}{Q_d} + \frac{1}{Q_{sw}} \tag{2.8}$$

where

Q_t = total quality factor

Q_{rad} = quality factor due to radiation (space wave) losses

Qc = quality factor due to conduction losses

Q_d = quality factor due to dielectric losses

Q_{sw} = quality factor due to surface waves

For very thin substrates, the losses due to surface waves are very small and can be neglected. However, for thicker substrates they need to be taken into account.

The bandwidth is inversely proportional to the square root of the dielectric constant of the substrate and Q value is inversely related to bandwidth. Generally, MSAs have narrow bandwidth (BW), as a result of high Q value, typically 1–5%, which is the major limiting factor for the widespread application of these antennas. Increasing the height of substrate increases the BW but doing this will increase the fringing effect in MSAs [8], so this field has been the major thrust of research, and broad BW up to 70% has been achieved.

2.2 Introduction – FINITE ELEMENT METHOD

Computer Simulation Technology (CST) which is an antenna design simulation tool offers accurate, efficient computational solutions for electromagnetic design and analysis. It is user-friendly 3D EM simulation software enables us to choose the most appropriate method for the design and optimization of devices operating in a wide range of frequencies. It is based on Finite Element Method (FEM). FEM has its origin in the field of structural analysis. It is a more powerful and adaptable numerical technique for handling programs involving complex

geometries. In mathematics, FEM is a numerical technique for finding approximate solutions to boundary value problems. It uses variational methods (the Calculus of variations) to decrease an error function and produce a steady solution. As we know that joining many tiny straight lines can approximate a larger circle, FEM involves all the methods for connecting many simple element equations over many small subdomains, named finite elements, to approximate a more complex equation over a larger domain. FEM analysis of any problem involves basically four steps [15]:

- Discretizing the solution region into a finite number of sub-regions or elements.
- Deriving governing equations of the typical element.
- Assembling of all elements in the solution region.
- Solving the system of equations obtained.

Typical steps mentioned above are followed for numerical analysis to analyse and solve any complex structure. To represent any complex geometry, the geometry is sub-divided into many small regions called *finite elements* and equations are obtained for each finite element. After obtaining all the finite element's equations, they are recombined to get the global system of equations for final calculation of whole complex geometry. The global system of equations has known solution techniques, and can be calculated from the initial values of the original problem to obtain a numerical answer. The global system of equations has known solution techniques, and can be calculated from the initial values of the original problem to obtain a numerical answer. The sectoring of a total domain into smaller domains has several advantages:

- Complex geometry is represented exactly
- Different material properties is also included

- Total solution is easily represented
- Internment of local effects

Including these advantages, another advantage of FEM is that it is numerically stable method i.e. errors in the input and intermediate calculations do not accumulate, which avoids the resulting output to become meaningless.

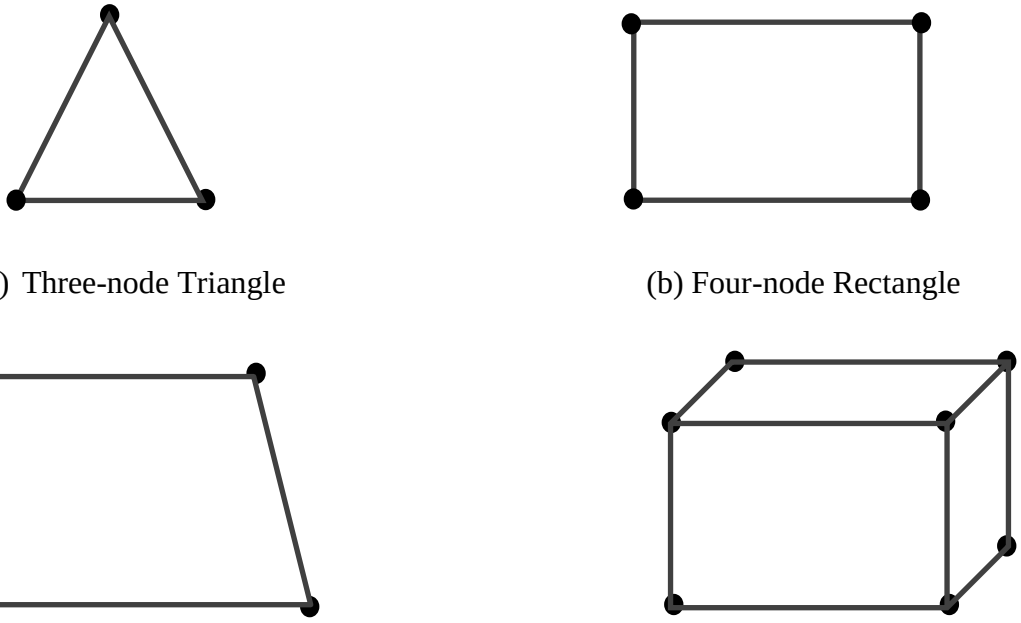

(a) Three-node Triangle (b) Four-node Rectangle

(c) Four-node Trapezium (d) Eight-node Hexahedron

Figure 2.13 Typical finite elements: (a)-(c) Two-dimensional, (d) Three-dimensional

The different finite elements are represented by different quadrilateral structures, few of them are shown in Fig. 2.13.

These structures are used to divide solution region into smaller parts having different number of nodes. In practical situations, however, it is preferred, for ease of computation, to have elements of same type throughout the region. Also, in view of the fact that quadrilateral elements do not conform to curved boundary as easily as triangular elements, we prefer to use triangular elements throughout our analysis. As triangular elements are having minimum

number of nodes compared to other quadrilateral, so we prefer triangle than other quadrilateral to have lesser complexity in calculation of potential at each nodes.

2.2.1 Finite Element Discretization

As an application to FEM to electrostatic problems, let us apply the four steps mentioned is the process of FEM solution to solve Laplace equation, $\nabla^2 V = 0$.

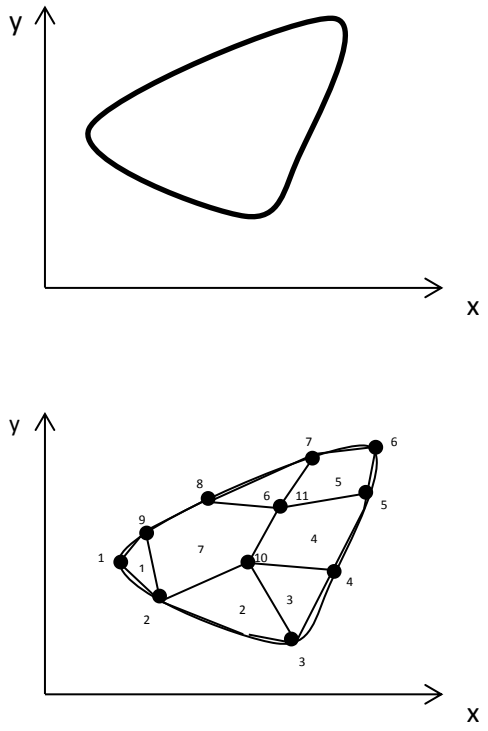

(a) Solution

(b) Finite Element Discretization

Figure 2.14 (a) Solution Region (b) Finite Element Discretization

Fig. 2.14(a) shows a region whose analysis has to be done by FEM. To obtain the potential distribution V(x, y) for the two-dimensional solution region the solution region is divided into many smaller sub-regions called finite-elements as shown in Fig. 2.14(b). The solution region is divided into seven non-overlapping finite elements, one of them is five-node quadrilateral, some are four-node quadrilaterals and rest are three-node triangles. In practical situations, elements of same type throughout the region are preferred as it will ease the computation. In view of the fact that quadrilateral elements do not conform to curved boundary as easily as

triangular elements, we prefer to use triangular elements throughout our analysis. So we will split four-node quadrilateral to two three-node triangles, so we have twelve triangular regions of the whole solution regions.

To find the potential of whole solution region V(x,y), we will start to find potential of each node $V_e(x,y)$ of each triangular element and then interrelate the potential distribution in various elements such that the potential is continuous across inter-element boundaries. The approximate solution for the whole region is [15]

$$V(x,y) \cong \sum_{e=1}^{N} V_e(x,y) \tag{2.9}$$

where N is the number of triangular elements into which the solution region is divided. The most common form of approximation for V_e within an element is polynomial approximation, namely,

$$V_e(x,y) = a + bx + cy \tag{2.10}$$

for triangular element and

$$V_e(x,y) = a + bx + cy + dxy \tag{2.11}$$

for quadrilateral element. The constants a, b, c and d are to be determined. The potential V_e in general is non-zero within element *e* but zero outside *e*.

$$E_e = -\nabla V_e = -(ba_x + ca_y) \tag{2.12}$$

2.2.2 Element Governing Equations

A typical triangular element is considered. The potentials V_{e1}, V_{e2} and V_{e3} at node 1, 2 and 3, respectively are obtained in [16] by using Eq. 2.10:

$$\begin{bmatrix} V_{e1} \\ V_{e2} \\ V_{e3} \end{bmatrix} = \begin{bmatrix} 1 & x_1 & y_1 \\ 1 & x_2 & y_2 \\ 1 & x_2 & y_3 \end{bmatrix} \begin{bmatrix} a \\ b \\ c \end{bmatrix} \tag{2.13}$$

The coefficients a, b and c are determined by above equation as

$$\begin{bmatrix} a \\ b \\ c \end{bmatrix} = \begin{bmatrix} 1 & x_1 & y_1 \\ 1 & x_2 & y_2 \\ 1 & x_2 & y_3 \end{bmatrix}^{-1} \begin{bmatrix} V_{e1} \\ V_{e2} \\ V_{e3} \end{bmatrix} \tag{2.14}$$

$$V_e = [1 \quad x \quad y] \frac{1}{2A} \begin{bmatrix} (x_2y_3 - x_3y_2) & (x_3y_1 - x_1y_3) & (x_1y_2 - x_2y_1) \\ (y_2 - y_3) & (y_3 - y_1) & (y_1 - y_2) \\ (x_3 - x_2) & (x_1 - x_3) & (x_2 - x_1) \end{bmatrix} \begin{bmatrix} V_{e1} \\ V_{e2} \\ V_{e3} \end{bmatrix}$$

$$V_e = \sum_{i=1}^{3} \alpha_i(x,y)\, V_{ei} \tag{2.15}$$

where

$$\alpha_1 = \frac{1}{2A} [(x_2y_3 - x_3y_2) + (y_2 - y_3)x + (x_3 - x_2)y], \tag{2.16a}$$

$$\alpha_2 = \frac{1}{2A} [(x_3y_1 - x_1y_3) + (y_3 - y_1)x + (x_1 - x_3)y], \tag{2.16b}$$

$$\alpha_3 = \frac{1}{2A} [(x_1y_2 - x_2y_1) + (y_1 - y_2)x + (x_2 - x_1)y] \tag{2.16c}$$

where A is area of the element

$$2A = \begin{bmatrix} 1 & x_1 & y_1 \\ 1 & x_2 & y_2 \\ 1 & x_2 & y_3 \end{bmatrix}$$

$$= (x_2y_3 - x_3y_2) + (x_3y_1 - x_1y_3) + (x_1y_2 - x_2y_1)$$

or,

$$A = \frac{1}{2} [(x_2 - x_1)(y_3 - y_1) - (x_1 - x_3)(y_1 - y_2)] \tag{2.17}$$

If the nodes are numbered counter-clockwise then the value of A is positive as shown in Fig. 2.15.

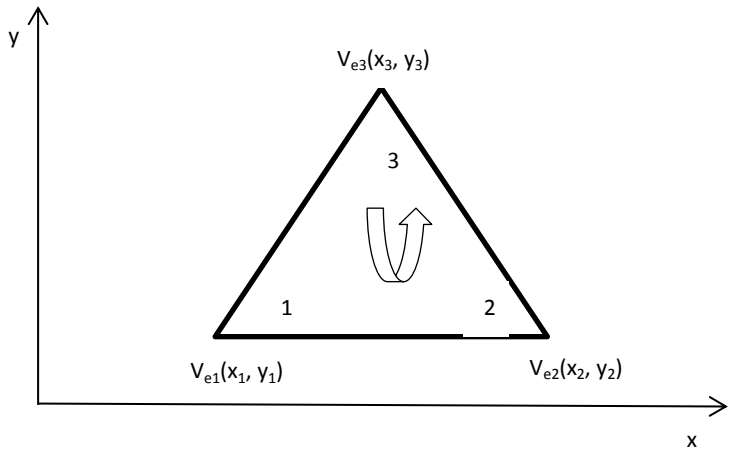

Figure 2.15 Triangular element with node numbering anti-clockwise

Eq. 2.15 provides the potential at any point (x, y) within the element provided that the potentials at the vertices are known.

Linear interpolation functions are given by α_i. They are called the *element shape functions* and they have following properties [17]:

$$\alpha_i = \begin{cases} 1, & i = j \\ 0, & i \neq j \end{cases} \tag{2.18a}$$

$$\sum_{i=1}^{3} \alpha_i(x, y) = 1 \tag{2.18b}$$

The functional corresponding to Laplace's equation is given by

$$W_e = \frac{1}{2} \int \in |E_e|^2 \, ds = \frac{1}{2} \int \in |\nabla V_e|^2 \, dS \tag{2.19}$$

$$\nabla V_e = \sum_{i=1}^{3} V_{ei} \nabla \alpha_i \tag{2.20}$$

Substituting Eq. 2.20 into Eq. 2.19 gives

$$W_e = \frac{1}{2} \sum_{i=1}^{3} \sum_{j=1}^{3} \epsilon \left[\int \nabla \alpha_i \, . \nabla \alpha_j \, dS \right] V_{ej} \tag{2.21}$$

Now we define a term as

$$C_{ij}^{(e)} = \int \nabla \alpha_i \, . \nabla \alpha_j \, dS \tag{2.22}$$

So Eq. 2.21 can be written in matrix form as

$$W_e = \frac{1}{2} \in [V_e]^t \left[C^{(e)}\right] [V_e] \tag{2.23}$$

where the subscript *t* denotes the transpose of a matrix,

$$\left[C^{(e)}\right] = \begin{bmatrix} C_{11}^{(e)} & C_{12}^{(e)} & C_{13}^{(e)} \\ C_{21}^{(e)} & C_{22}^{(e)} & C_{23}^{(e)} \\ C_{31}^{(e)} & C_{32}^{(e)} & C_{33}^{(e)} \end{bmatrix} \tag{2.24}$$

The matrix $[C^{(e)}]$ is called as *element coefficient matrix*. The element $C_{ij}^{(e)}$ of the coefficient matrix is regarded as the coupling between nodes i and j; its value is obtained from Eqs. 2.16 & 2.22.

For example,

$$C_{12}^{(e)} = \int \nabla\alpha_1 \,.\, \nabla\alpha_2 \, dS$$

$$= \frac{1}{4A^2}[(y_2 - y_3)(y_3 - y_1) + (x_3 - x_2)(x_1 - x_3)] \int dS$$

$$= \frac{1}{4A}[(y_2 - y_3)(y_3 - y_1) + (x_3 - x_2)(x_1 - x_3)] \tag{2.25}$$

Similarly, all the coefficients are obtained.

Also,

$$C_{21}^{(e)} = C_{12}^{(e)}, C_{31}^{(e)} = C_{13}^{(e)}, C_{32}^{(e)} = C_{23}^{(e)} \tag{2.26}$$

2.3 Summary

This chapter has discussed about the characteristics of microstrip antennas. This chapter has also given insight of small and compact antennas with different feeding mechanism that is required for wireless applications. The need of 50Ω transmission line has also been discussed. It has deduced the complete theory behind the design of microstrip

antenna with their advantages and disadvantages. The structural analysis by FEM technique has been briefly explained. A number of equations are analyzed to give insight into the structural behavior of the microstrip antennas.

CHAPTER 3

FRACTAL ANTENNA

FRACTAL ANTENNA

3.1 Introduction

Fractal is a concept which is being implemented in microstrip antenna to have better characteristics than microstrip antenna. The word fractal is derived from the Latin word "fractus" meaning broken, uneven, any of various extremely irregular curves or shape that repeat themselves at any scale on which they are examined. Using fractal in an antenna maximizes the length, or increase the perimeter (on inside sections or the outer structure), of material that can receive or transmit electromagnetic radiation within a given total surface area or volume. Rumsey, a well-known scientist, established that an antenna with shapes only defined by angles would be frequency independent, since it would not have any characteristics size to be scaled with wavelength. The term "fractal" was first used by mathematician Benoit Mandelbrot in 1975 [18]. He was sometimes referred to as the father of fractal geometry, who said, "I coined fractal from the Latin adjective *fractus*".

In many fractal antennas, the self-similarity and plane-filling nature of fractal geometries are often quantitatively linked to its frequency characteristics. Fractals are geometrical shapes, which are self-similar, repeating themselves at different scales. The geometry of fractals is important because the effective length of the fractal antennas can be increased while keeping the total area same. The shape of fractal antenna can be formed by an iterative mathematical process called, *Iterative Function Scheme* (IFS) which will be discussed later in this chapter. There are different types of fractals which reveal that as you zoom in on the image at finer and finer scales, the same pattern re-appears so that it is virtually impossible to know at which level you are looking.

The geometry of fractals is important because the effective length of the fractal antenna can be increased while keeping the total area same. Fractal antenna design has two things:

1) *Initiator (0^{th} stage):* It is basic shape of the geometry. It can be any shape either triangle, rectangle or any other quadrilateral.

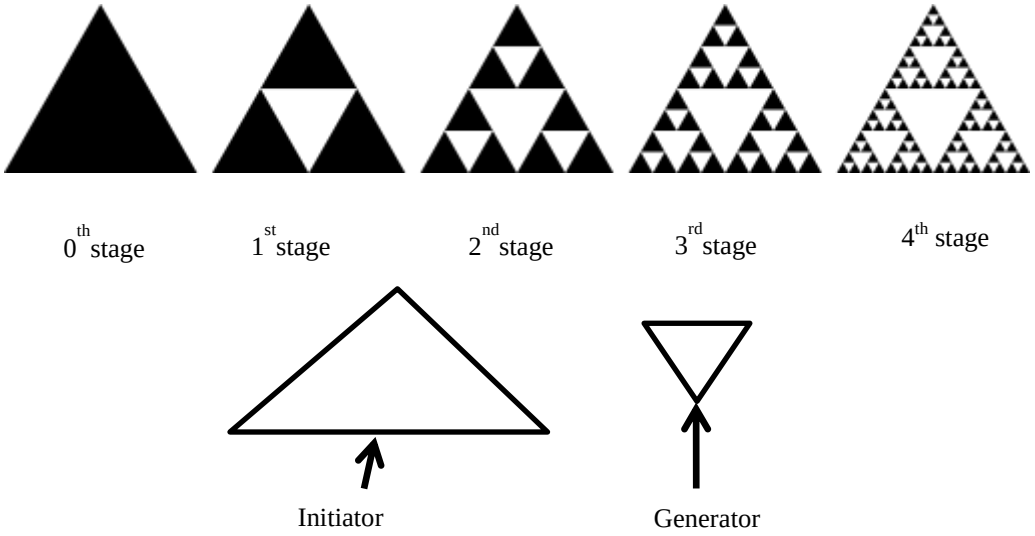

Figure 3.1 Sierpinski Gasket with subsequent stages showing initiator and generator

2) *Generator*: It is the shape which is obtained by scaling the initiator and will be repeated either inside or outside on the initiator to obtain subsequent stages to reach final fractal geometry. Generator is obtained from the initiator itself.

In Fig. 3.1 showing one type of fractal geometry which is named as *Sierpinski Gasket* which is derived by taking a triangular geometry as initiator and repeating a down-scaled version of initiator called generator inside it to obtain subsequent stages of gasket.

3.1.1 Features of Fractal

There are many features of fractal antenna which make them useful for many applications. Some of them are tabulated in Table 3.1.

Table 3.1 Features of fractal antennas

Self-Similarity	Useful in designing multi-band antenna.
Small Dimension	Useful to design electrically small antennas.
Space-Filling Ability	Useful for miniaturization of an antenna by increasing the electrical length into a compact physical volume.
Increasing number of Iterations	Useful to decrease the resonant frequency while electrical length increases.
Sharp Edges, Corners and Discontinuities	Helps to make antenna to radiate efficiently.

Other important factors that are differentiating it with microstrip antennas are:

- Fractals are having no characteristics shape.
- They have infinite range of scales within their structure, being composed of an infinite number of clusters which are equal to the whole shape but to a smaller scale.
- They are highly convoluted and having irregular shapes.
- Since characteristic size has to be avoided to design a frequency independent antenna or at least the antenna structure has to include many characteristics sizes to allow a multi-wavelength operation and fractal antenna has this property to become a good candidate for becoming frequency independent.

Fractals are structure of infinite complexity with a self-similar nature. It means that as the structure is zoomed in upon, the structure repeats itself. This property could be used to design antennas that can operate at several frequencies.

Fractal can fill the space occupied by the antenna in a more effective manner than the traditional Euclidean geometry antenna. This can lead to more coupling of energy from transmission lines to free space in less volume. It has a large number of irregularities, which results in virtually infinite physical length. At higher frequencies, these antennas are naturally

broadband. The basic difference between traditional Euclidean geometry and fractals are discussed in Table 3.2.

Table 3.2 Fractal vs. Euclidean geometry

Fractal geometry	**Euclidean geometry**
10-20 years old	$>$ 2,000 years old
Defined by iterative rule	Defined by formula
Structure on many scales	Structure on one or few scales
Dilation or self-similarity property	No self-similarity
Fractional dimension possible	Finite dimension
Long range correlation	Variable correlation
Rough on most scales	Smooth on most scales

3.1.2 Classes of Fractals

There are different classes of fractals described in a flow chart form in Fig. 3.2. There are basically two classes of it named as *Deterministic* and *Non- Deterministic*. Our point of discussion in this chapter is Deterministic fractals which are again characterized as *Linear* and *Non-Linear* geometry. Linear geometry is derived by using *Iterative Function System* (IFS) which is main topic of discussion in this chapter. Under Linear geometry, there are many curves so-called fractal curves such as *Koch curve, Cantor curve, Minkowski curve, Sierpinski gasket* and many more. These are explained one by one below.

- **Koch curve**: It is a good example of self-similar space-filling fractals which have been used to develop wideband/multiband and/or miniaturized antennas [16]. The features of the Koch geometry can overcome some of the limitation of small antennas [20]. The expected benefit of using a fractal as a dipole antenna is to miniaturize the total height of antenna at resonance. This is achieved by using Koch geometry. It does

not have piecewise continuous derivative. It is nowhere differentiable. Its shape is highly rough and uneven. So works as a very efficient radiator as shown in Fig. 3.3(a).

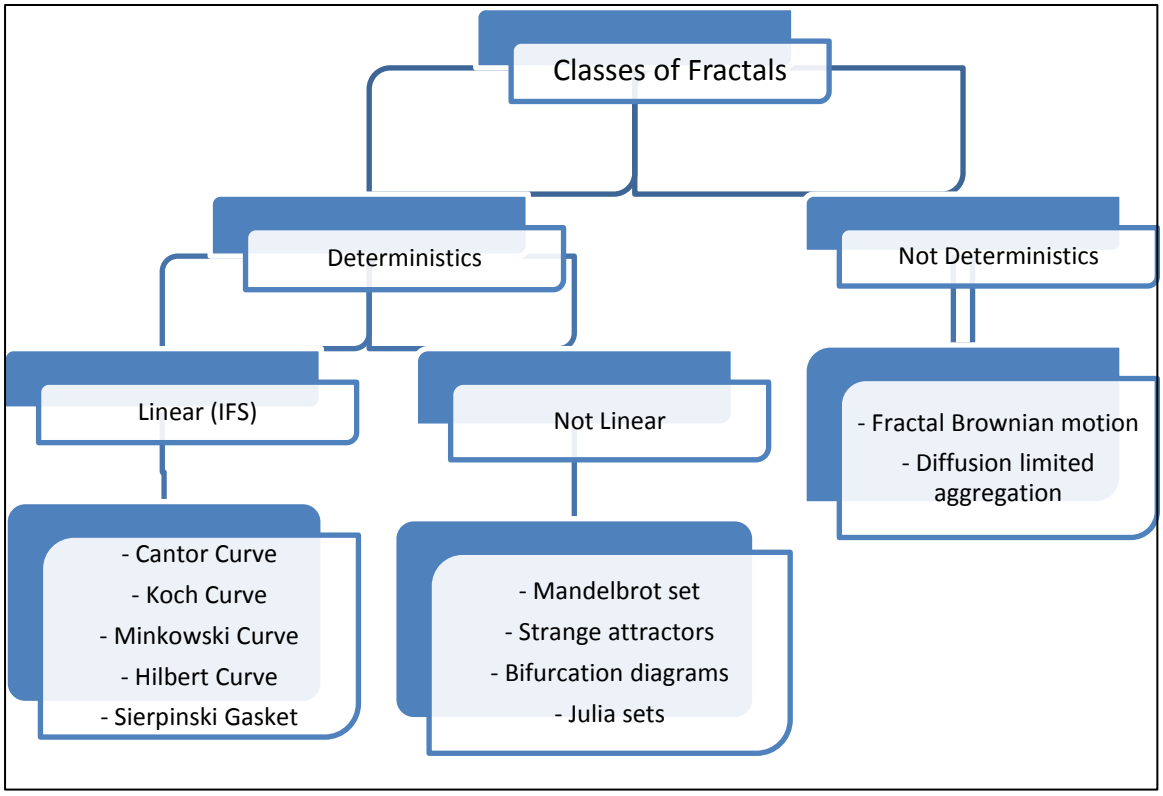

Figure 3.2 Classes of fractals

- **Minkowski loop:** It can be used to reduce the size of antenna by increasing the efficiency with which fills up occupied volume with electrical length. It is analysed where the perimeter is one wavelength. Several iterations are compared with a square loop antenna to illustrate the benefits of using fractal antenna [21]. It is shown in Fig. 3.3(b). It is interesting to note that Minkowski fractal antennas are not only broadband, but they also demonstrate multiband effects. This is due to the coupling between the wires. As more contours and iterations of the fractal are added, the coupling becomes more complicated and different segments of the wire resonate at different frequencies. Minkowski island fractals can be used to achieve

miniaturization in antenna systems while keeping an identical electromagnetic performance to the square loop antenna [22].

- **Sierpinski gasket:** It was discovered by Polish mathematician Waclaw Sierpinski in 1916. The Sierpinski sieve of triangles possesses a certain multiband behavior owing to its self-similar shape as shown in Fig. 3.3(c). A multiband fractal monopole antenna [23], based on the Sierpinski gasket, was first introduced by Puente et al. [24]. The Sierpinski triangle has *Hausdorff* dimension $\log(3)/\log(2) \approx 1.585$, which follows from the fact that it is a union of three copies of itself, each scaled by a factor of 1/2. The area of a Sierpinski triangle is zero. The area remaining after each iteration is clearly 3/4 of the area from the previous iteration, and an infinite number of iterations results in zero [25].
- **Fractal loops:** Loop antennas are well understood and have been studied using a variety of Euclidean geometry. Fractal loop antennas have shown improved impedance and SWR performance in a reduced physical area when compared to non-fractal Euclidean geometries [26]. Resonant loop antennas require a large amount of space and small loops have very low input impedance. A fractal island can be used as a loop antenna to overcome these drawbacks. It has the property that the perimeter increases to infinity while maintaining the volume occupied. For small loop this increase in length improves the input resistance, thereby antenna can be more easily matched to a feeding transmission line as shown in Fig. 3.3(d).
- **Cantor Set:** The Cantor set is a set of points lying on a single line segment that has a number of remarkable and deep properties. It was discovered by H. J. S. Smith in 1874 and introduced by German mathematician Georg Cantor in 1883. It is obtained by taking out the one-third part of a unit length line (line can be of different

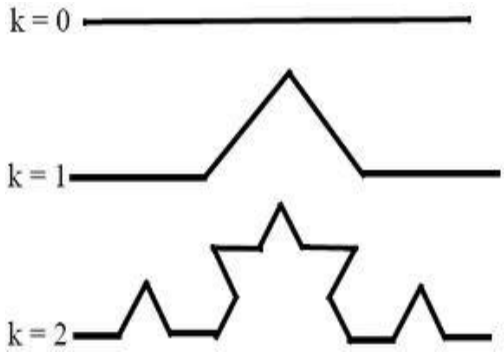

(a)

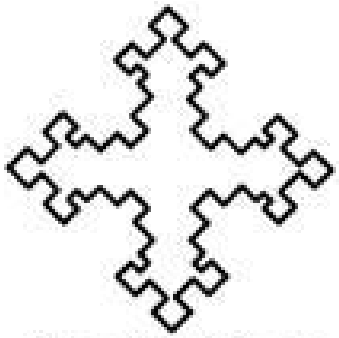

(b)

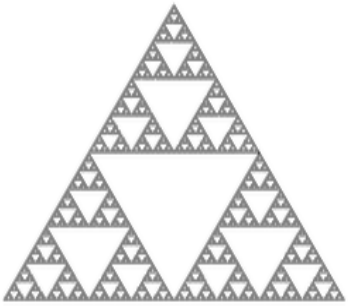

(c)

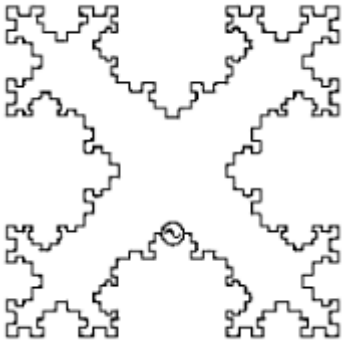

(d)

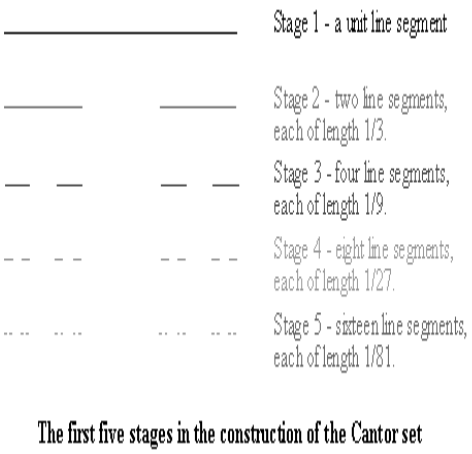

(e)

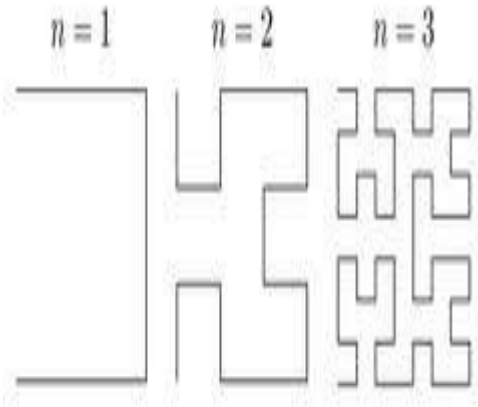

(f)

Figure 3.3 Different fractal geometries (a) Koch curve, (b) Minkowski Loop, (c) Sierpinski Gasket, (d) Fractal loop, (e) Cantor set and (f) Hilbert Curve

dimensions) at each iterated occasion as described by Fig. 3.3(e). The different wideband cantor set antenna has been proposed in [27, 28].

- **Hilbert Curve:** The space-filling properties lead to curves that are electrically very long, but fit into a compact physical space. This property leads to miniaturization of antenna. Hilbert curve is one of the fractal curves which are having this property [29]. Because of this property it has become an attractive candidate for use in the design of fractal antennas. The first little iteration of Hilbert curves are shown in Fig. 3.3(f). It may be noticed that each successive stage consists of four copies of the previous, connected with additional line segments. This geometry is a space-Filling curve, since with a larger iteration, one may think of it as trying to fill the area it occupies. Additionally the geometry also has the following properties: Self-Avoidance (as the line segments do not intersect each other), Simplicity (since the curve can be drawn with a single stroke of a pen) and Self-Similarity. Because of these properties, these curves are often called as FASS curves [30]. The space-filling properties of the Hilbert curve we investigated in [31, 32].

3.1.3 Fractal Dimensions

Generally, we can think of objects that are zero dimensional (0-D) i.e. points, 1-D i.e. lines, 2-D i.e. planes and 3-D i.e. solids. We are known with zero, one, two and three dimensions. But for fractal antenna, we will talk about fractal dimensions i.e. non-integer dimensions, such as 2.12D, 1.14D, 3.79D, etc. There are many fractal dimensions; some of them will be discussed here.

Few of the fractal dimensions are *Similarity dimension* (DS), *the Hausdorff Dimension* (DH), *Box-counting dimension* (DB), etc. We will mostly concentrate on similarity dimension (DS), to characterize the construction of regular fractal objects. Fractals are characterized by their dimension. It is the key structural parameter describing the fractal and is defined by partitioning the volume where the fractal lies into boxes of side δ.

3.1.3.1 Similarity Dimension

The concept of dimension is closely associated with that of scaling. Consider a line is divided into N smaller self-similar segments, each ‘δ’ in length, then δ is in the scaling ratio. Thus,

For unit line $L = N\delta = 1$ (3.1)

For unit area $A = N\delta^2 = 1$ (3.2)

For unit volume $V = N\delta^3 = 1$ (3.3)

Therefore we see that the exponent of δ in each case is a measure of the dimension of the object. Thus

$$N\delta^{DS} = 1 \quad (3.4)$$

Therefore $$DS = \frac{\log N}{\log (\frac{1}{\delta})} \quad (3.5)$$

where DS denotes the similarity dimension.

For Cantor Set, there are two such identical copies of the set contained within the set.

So, N = 2 and $\delta = \frac{1}{3}$.

Hence $$DS = \frac{\log 2}{log\ 3} = 0.6309 \quad (3.6)$$

So, for Cantor Set, $0 < DS < 1$, that is it has a non-integer similarity dimension of 0.6309; due to fractal structure of the object.

3.1.4 Iterative Function System

Iterative function schemes (IFS) represent an extremely versatile method for conveniently generating a wide variety of useful fractal structures. These iterated function systems are based on the application of a series of affine transformations, w, defined by [23]

$$w\begin{pmatrix}x\\y\end{pmatrix} = \begin{pmatrix}a & b\\c & d\end{pmatrix}\begin{pmatrix}x\\y\end{pmatrix} + \begin{pmatrix}e\\f\end{pmatrix} \tag{3.7}$$

or, $$\mathrm{w}\,(\mathrm{x},\,\mathrm{y}) = (ax + by + e, cx + dy + f) \tag{3.8}$$

where a, b, c, d, e and f are real numbers. Hence, the affine transformations, w, is represented by six parameters

$$\left(\begin{array}{cc|c}a & b & e\\c & d & f\end{array}\right) \tag{3.9}$$

whereby a, b, c, an d control rotation and scaling, while e and f control linear translation [25].

Now suppose we consider w_1, w_2, …., w_N as a set of affine linear transformations, and let A be the initial geometry. Then a new geometry, produced by applying the set of transformations to the original geometry, A, and collecting the results from $w_1(A)$, $w_2(A), \ldots, w_N(A)$, can be represented by

$$W(A) = \bigcup_{n=1}^{N} w_n(A) \tag{3.10}$$

where W is known as the Hutchinson operator [33, 34].

A fractal geometry can be obtained by repeatedly applying W to the previous geometry. For example, if the set A_o represents the initial geometry, then we will have

$$A_1 = W(A_o); A_2 = W(A_1); \ldots\ldots; A_{k+1} = W(A_k) \tag{3.11}$$

An iterated function system generates a sequence that converges to a final image, A_∞, in such a way that

$$W(A_\infty) = A_\infty \tag{3.12}$$

This image is called attractor of the iterated function system, and represents a "fixed point" of W.

3.1.5 Advantages and Disadvantages of using Fractals

There are countless advantages and some disadvantages as well of using fractals in microstrip antennas. They are discussed in detail in the subsections below.

3.1.5.1 Advantages

The advantages of using fractals in microstrip antenna are illustrated in here. Some of them are:

- Size can be shrunk from two to four times with surprising good performance.
- Multiband performance is at non-harmonic frequencies.
- Compressed resonant behaviour.
- At higher frequencies the finite element antenna is naturally broadband.
- Improved reliability
- Reduced construction costs.
- Polarisation and phasing of FEA also are possible.
- Because FEA are self-loading, no antenna tuning coils or capacitors are necessary.
- They do not require any matching components to achieve multiband or broadband performance.

3.1.5.2 Disadvantages

With a number of advantages of using fractals in microstrip antenna, there are some disadvantages associated with it too. They are as follows:

- Low Gain
- Too complex geometry
- Numerical Limitations
- Practically only few iterations are possible to design, after that benefits start to diminish.

3.2 Summary

This chapter has discussed about fractal geometry. Fractal antenna engineering represents a relatively new field of research that combines attributes of fractal geometry with antenna theory. Fractals are space-filling geometries that can be used as antennas to effectively fit long electrical lengths into small areas. Iterative function schemes (IFS) with different fractal dimensions has been discussed. IFS represent an extremely versatile method for conveniently generating a wide variety of usual fractal structures. The performance of the fractal antenna with respect to conventional Euclidean geometry has also been discussed.

CHAPTER 4

WIDEBAND ANTENNA DESIGN

WIDEBAND ANTENNA DESIGN

This chapter surveys a planar monopole antenna using the Hexagonal Gasket. The design demonstrates details of fractal geometries developed to get wideband behaviour of patch resonator antenna. Research on the performance of the antenna by creating iterated fractal hexagons to increase the total perimeter (electrical length) of patch antenna is presented. The behaviour of patch resonator for various incremental steps in fractions, results in significant improvement in bandwidth. A Slot is created in the ground plane to increase the matching and thus bandwidth further and slits are introduced to achieve a notch band at desired frequency. The designed fractal-like geometry is realized on a FR4 substrate of relative dielectric constant of 4.4 and 1.6mm of width with 50-ohm microstrip feedline for UWB application. The simulated results show that the antenna has a good performance with 10dB-return loss in the frequency range 2.64-6.96GHz that results in a fractional bandwidth (FBW) of 90%. In addition, antenna performances such as radiation patterns and antenna gains over the operating bands have been presented and compared with the measured results.

4.1 Introduction

In 2002, Federal Communication Commission (FCC) allocated the bandwidth 3.l-10.6GHz for commercial use and named it as UWB frequency band. UWB technology offers significant benefits for Government, public safety, businesses and consumers. The frequency band of operation is based on the –10 dB bandwidth of the UWB emission. It is believed that the greatest potential use of UWB is in short-range communications in the home or business, allowing equipment mobility and high data rates to facilitate information sharing. Some of UWB applications are ground penetrating radar (GPR) systems, wall-imaging systems,

automotive collision avoidance systems, radar level gauges used in storage tanks, and communications systems measurement systems [4].

In recent years, modern telecommunication systems require compact and small antennas with wider bandwidth rather than conventional ones. Many methods for the design of antennas are used for improving their performances. One of these methods is fractal and it is more efficient for antennas to expand the bandwidths and reduce the dimensions [35]. The fractal antennas are preferred because of their lightweight, small dimension and also the fact that they have extreme wideband characteristics [36]-[41]. Various antennas for wideband operation have been studied [42]-[43]. Fractals are recursively generated object having a fractional dimension. Fractals have space-filling property which leads to curves that are electrically very long, but fit into compact physical space. This property leads to the miniaturization of antenna elements. There are a variety of fractal shapes, such as Hilbert Curve [44], Sierpinski-carpet [45], Minkowski [21], Koch curve [19] etc.

This chapter illustrates a microstrip-fed monopole hexagonal shaped fractal antenna for UWB application. The design is implemented by doing fractal on base hexagonal patch till second iteration. The simulation is done by using full wave EM simulation software. The design process of proposed antenna is presented in the antenna design section. Following this section, various antenna parameters such as return loss, radiation characteristics and gain are discussed which is caused due to iterations on the patch and introduction of a slot and slits in the ground plane. The simulated results are verified with the measured results. This paper ends with a set of conclusions.

4.2 Antenna Design

The presented antenna consists of a hexagonal patch element mounted on a dielectric layer over a ground plane. The low cost fiberglass dielectric substrate FR4 is used having 1.5 mm

of height and a relative permittivity of 4.4, and it is fed by a 50-ohm micro-strip line. The radiating patch is planned by taking hexagon as a base structure called generator [25]. The generator is downscaled by a factor of two which is added to each side of base structure such that the center point of the smaller hexagon will coincide with the center point of the edge of the previous structure.

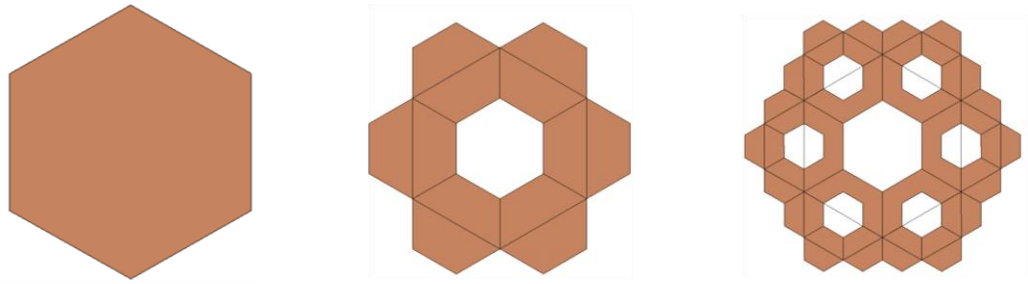

Figure 4.1 Geometry of the generator, 1st iteration and 2nd iteration

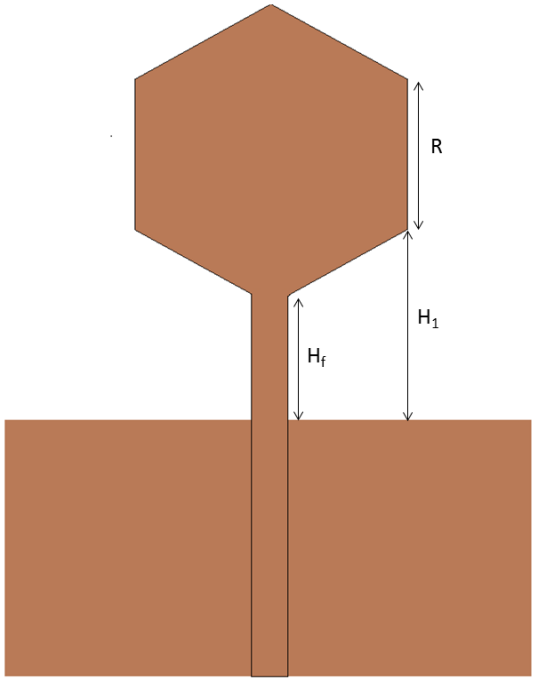

Figure 4.2 The generator with simple ground plane

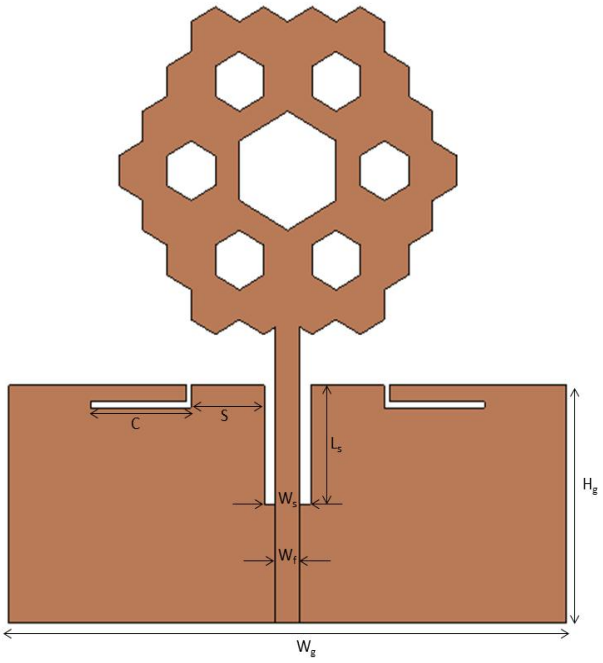

Figure 4.3 The presented antenna with modified ground plane

Later the hexagon formed inside the base structure because of this addition is removed to get1st iterated structure. Fig.4.1 shows the basic element and the iterated structures. Again the smaller hexagon is scaled down by 1/2 and the procedure is repeated to get 2nd and higher iterated structures. This process can be repeated upto countless iteration but practically infinite iterative structure is not possible because of fabrication constraints. The second iterative fractal antenna has been finalized to design. The detailed dimensions of the base antenna are as shown in Table 4.1.

Table 4.1: Dimension of the presented antenna (in mm)

R	H_1	H_f	W_g	H_g	W_s	L_s	W_f	S
10	10	5.635	50	20	4.2	10	2.2	6.56

The ground plane has been modified by introducing a slot of dimension $W_s \times L_s$ just beneath the 50-ohm microstrip line, Fig.4.3. Later an L-shaped narrow slit is introduced on the either side of the symmetry plane of the structure. The width of the slit is 0.5mm. The presented antenna with the discussed dimensions is fabricated and shown in Fig.4.4.

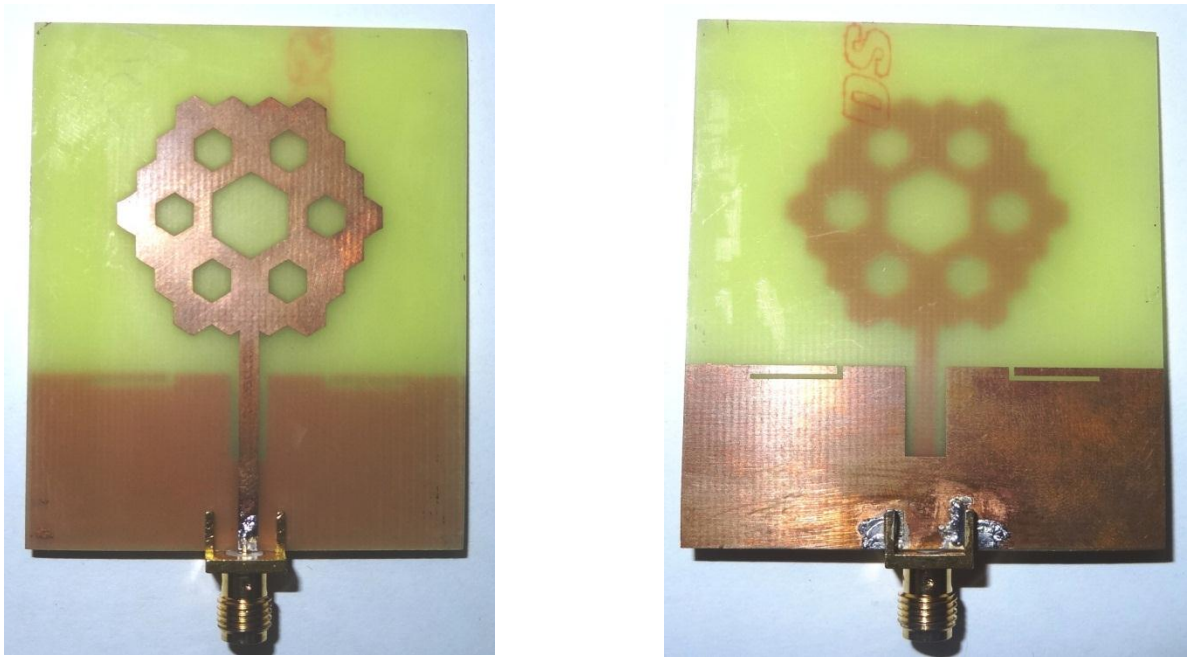

(a) (b)

Figure 4.4 Fabricated Antenna Image (a) Radiating Patch (b) Ground Plane

4.3 Anechoic Chamber

Anechoic Chamber is an antenna measurement chamber. It is a closed room having pyramidal-like arrangement on the side walls with conical shape facing outside the wall. All the walls of the room are coated with metals. This is done to avoid the outside radiation effect on the measurement of the test antenna. The pyramidal like dome shape is made to make the characteristic impedance to of atmosphere to match with the characteristic impedance of the Antenna under Test (AUT).

Chamber is having a positioner to fix the test antenna and the reference antenna is kept at other end having same polarization as that of the test antenna. The flowchart shown in Fig. 4.5 describes the measurement operation to be done to test the characteristics of the antenna. The source power is fed to the directional coupler which is distributed to amplifier and mixer. The power received by the amplifier is amplified and is fed to the reference antenna. This power will be radiated in the atmosphere inside the chamber and received by

the AUT. The power received by mixer from the directional coupler and AUT are compared to the Local Oscillator (LO) frequency to produce same Intermediate Frequency (IF) that is received by the receiver Rx. The positioner is connected to the positional controller that will control the axis and position of the AUT and a system (Computer) is linked to it to calculate the various results at different desired axis and position of the AUT.

There is basically four axis control system used for measurement. They are Azimuthal, Slide Roll and Elevation axis control system. Out of these, the first three control systems are used for main measurement and the last one is used for phase measurement.

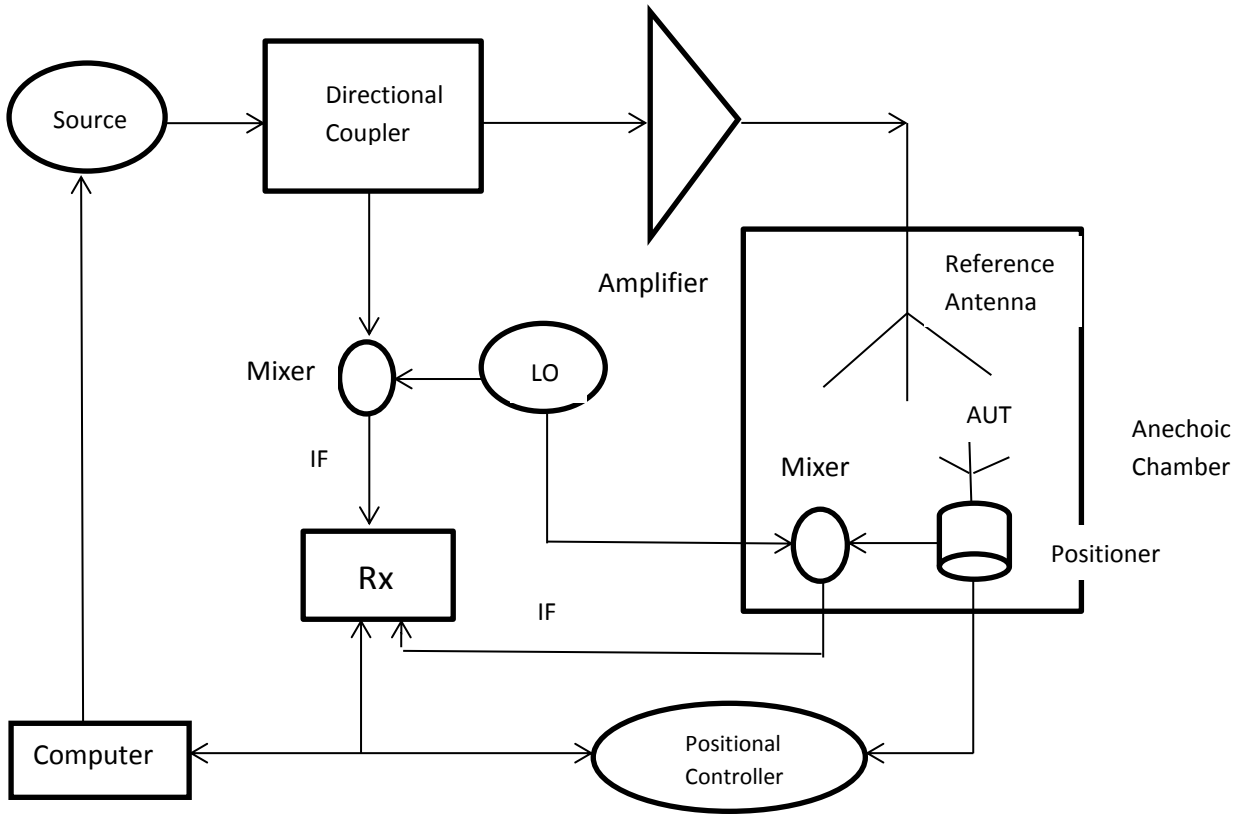

AUT- Antenna Under Test

IF- Intermediate Frequency

Figure 4.5 Anechoic Chamber Operation flowchart

4.4 Simulated and Measured Results

The given antenna is simulated and optimized by using a full wave EM simulator CST STUDIO SUITE. The simulated return loss against frequency for the proposed antenna is shown in Figs.4.6 & 4.7. In Fig.4.6, it is observed that as the iteration is done on the basic shape of patch antenna with simple ground plane, the whole band going downwards indicating increase in bandwidth.

As it is known that the bandwidth is inversely related to the Q-factor and the resonant frequency is directly related to the Q factor of the antenna. The Q of the antenna decreases with increase in the iteration number [46], therefore, the bandwidth gets wider and the resonant frequency decreases, shown in Fig. 4.6.

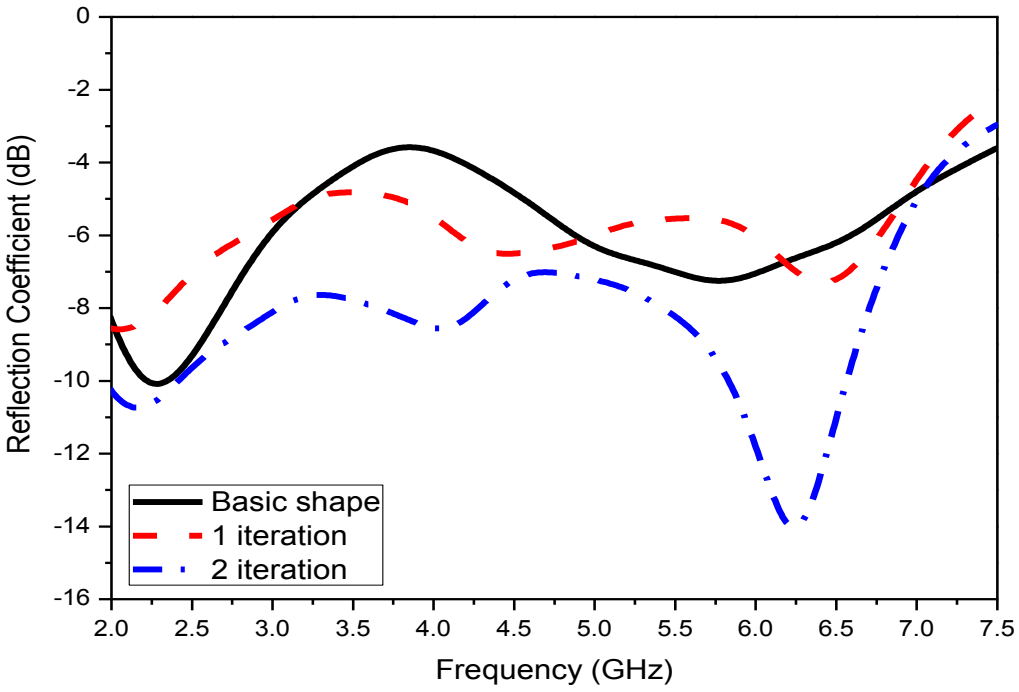

Figure 4.6. Return loss vs. level of iterations with simple ground plane

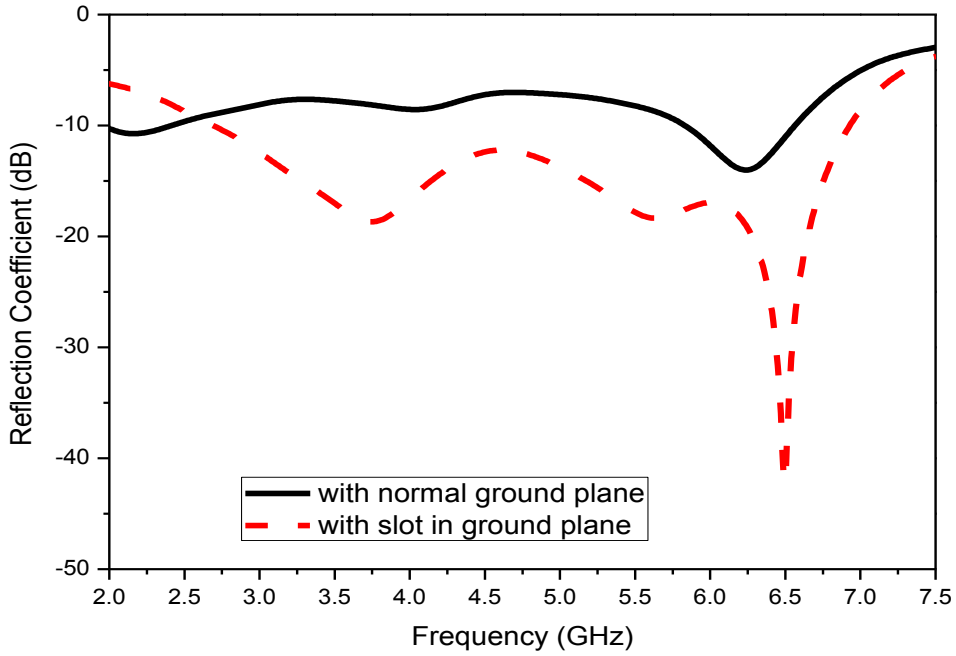

Figure 4.7 Return loss variation in 2nd iteration with slot in simple ground plane

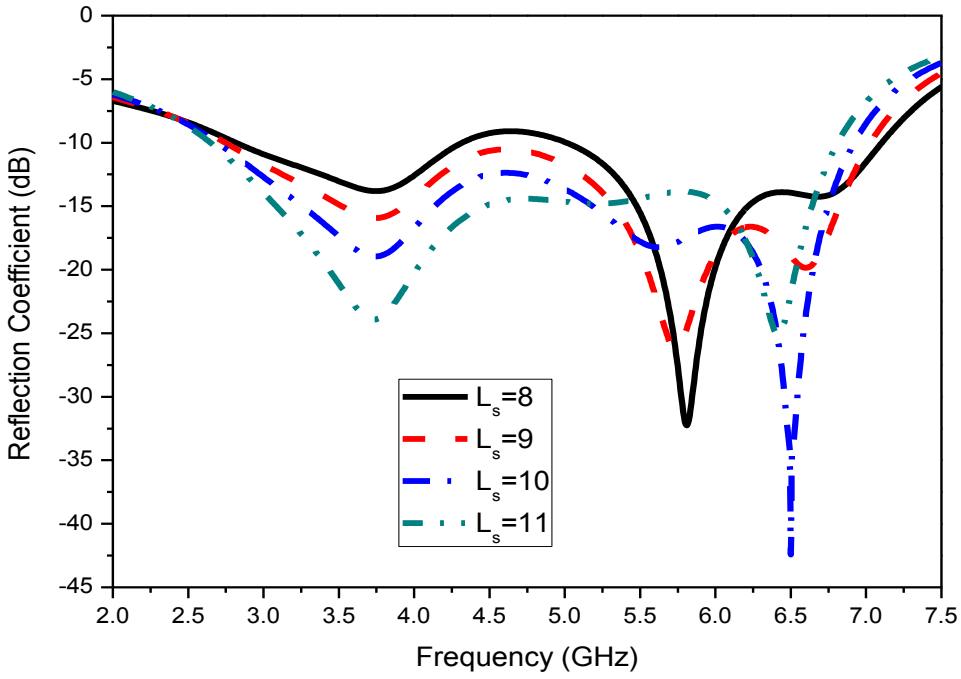

Figure 4.8 Return loss variation with different lengths of slot

Slot is introduced in the ground plane of the final second iterated structure for further improvement. The effect of the slot in the ground plane after the second iteration is illustrated in Fig. 4.7. An improved impedance matching is achieved for the whole band and the impedance bandwidth of the proposed antenna covers a wide operating band of 2.64-

6.96GHz with a FBW of 90% at the center frequency of 4.8GHz. The maximum return loss achieved is 12.2dB at 4.62GHz and the minimum return loss is 42dB at 6.5GHz. A parametric study has been done on lengths of slot from 8mm to 11mm with 1mm variation, shown in Fig. 4.8, and best value of return loss is found out to be 42dB at 6.5GHz for L_s=10mm which has been chosen for proposed design. Variation in width of slot is also done and optimized for the above value.

Finally, An L-shaped narrow slit of width 0.5mm and length of C is introduced on the either side of the symmetry plane of the structure to get a notched band characteristic. A parametric study has been done with the length of the slit and the effect of the slit length C is shown in Fig. 4.9. It can be seen that the notched band is tunable with C. As the length of the slit is varied from 8.5mm to 11.5mm with 1mm variation, the notch band gets shifted to lower frequency side as shown in Fig. 4.9. The relation between notched frequency and the slit length is given in Eq. 4.1.

$$f_{notch}(GHz) \approx \frac{v}{4C\sqrt{\varepsilon_{eff}}} \tag{4.1}$$

where,

v = velocity of light, m/s

C = length of slit in ground plane, mm

ε_{eff} = effective dielectric constant of substrate

The slit length is taken as 9.5mm to get notched band between 4.1-4.5GHz. A comparison has been shown for the gain of the antenna, Fig. 4.12, with and without slit. For the notched type the gain is 2.84dB at 3.8GHz which reduces to 0.899dB at 4.2GHz showing a notched band in that region. The maximum value of the gain is 5.2dB at 6.5GHz.

The measured result is compared with the simulated one and they are well matched as shown in Fig. 4.10. The slight deviation is produced by the error in the manufacturing and measurement. Fig. 4.11 displays the measured co-polarization and cross-polarization radiation patterns at different frequencies. The antenna is having broadside radiation pattern at all the operating frequencies as illustrated by Fig. 4.11.

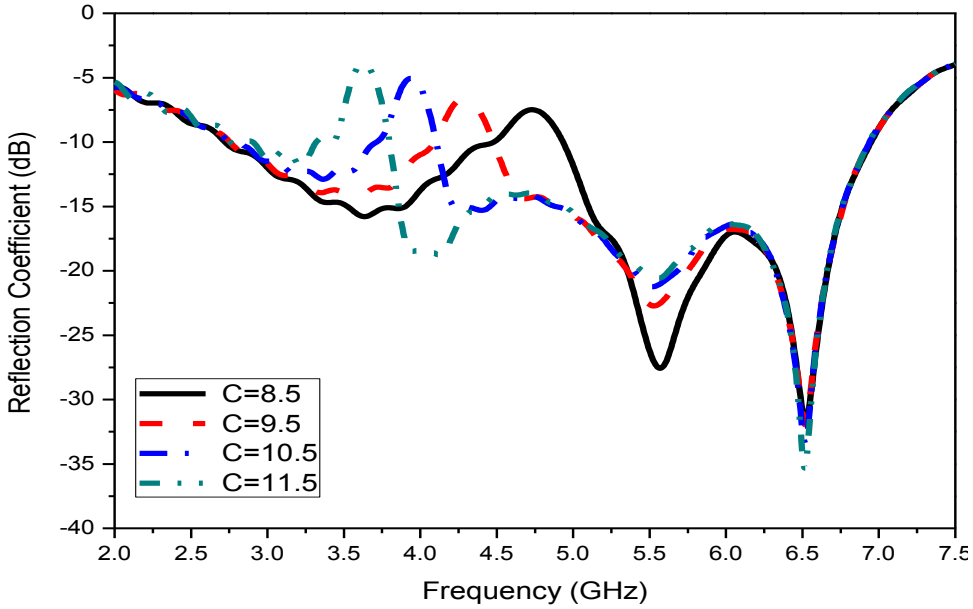

Figure 4.9 Variation in notched band with length of slit

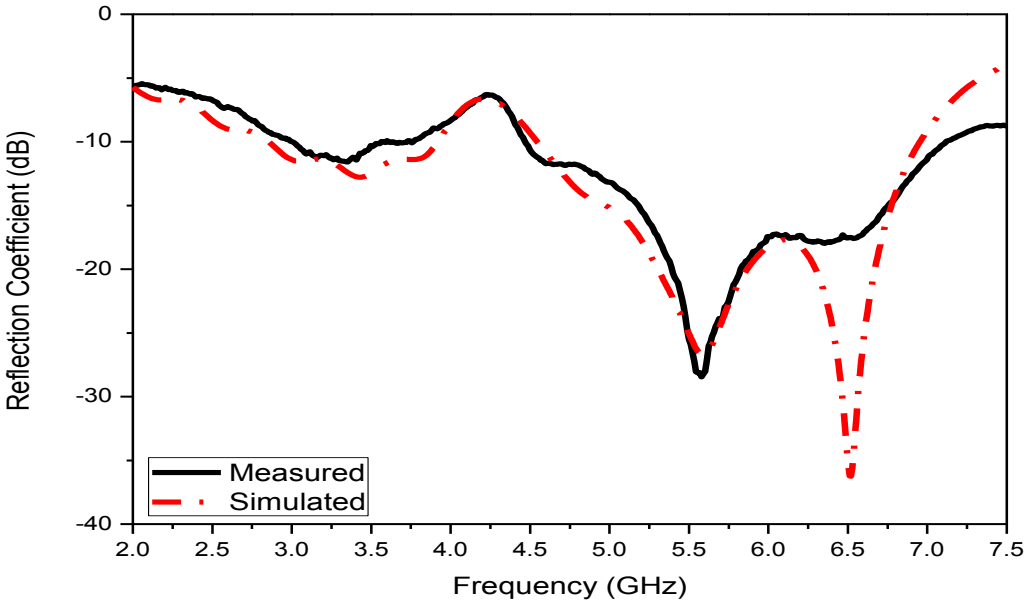

Figure 4.10 Measured vs. Simulated Return-Loss Characteristics

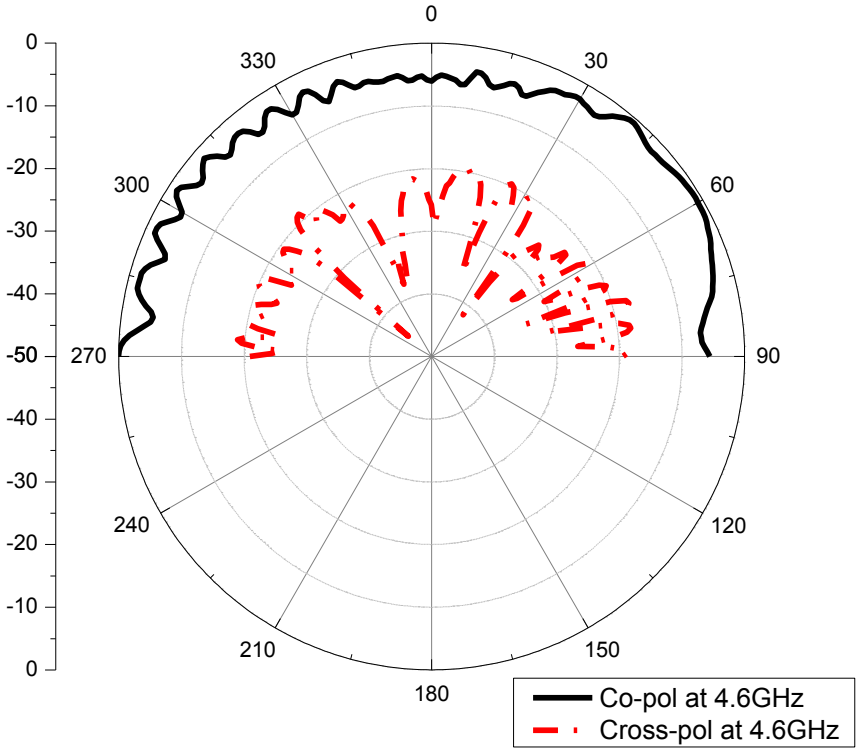
0
30
60
90
120
150
180
210
240
270
300
330
0
-10
-20
-30
-40
-50
-40
-30
-20
-10
0
Co-pol at 4.6GHz
Cross-pol at 4.6GHz

(a)

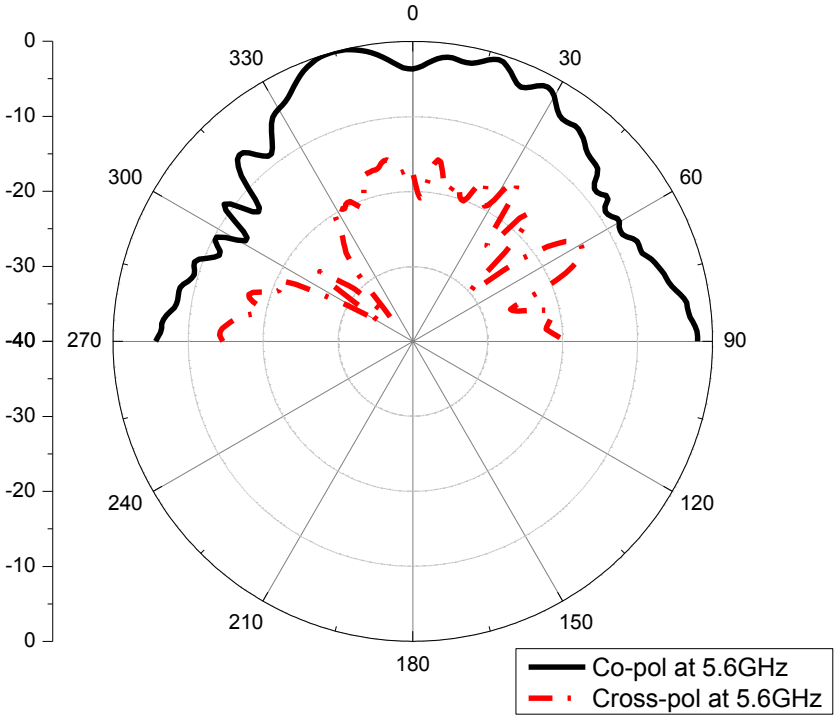
0
30
60
90
120
150
180
210
240
270
300
330
0
-10
-20
-30
-40
-30
-20
-10
0
Co-pol at 5.6GHz
Cross-pol at 5.6GHz

(b)

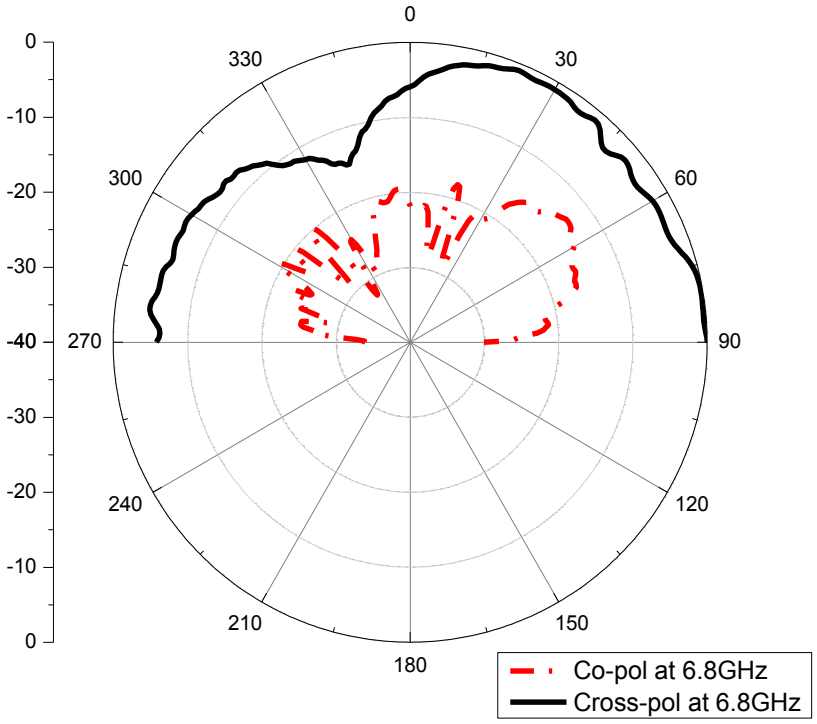

(c)

Figure 4.11. Measured Co-pol and Cross-pol field at (a) 4.6GHz (b) 5.6GHz (c) 6.8GHz

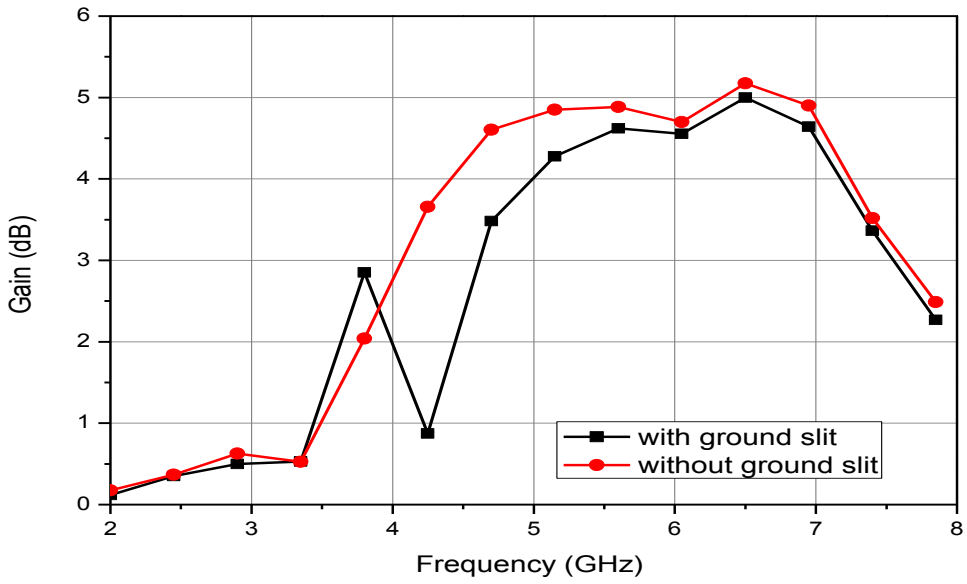

Figure 4.12 Simulated gain of the proposed antenna

The lower band-edge frequency for wideband antenna is described in [20], and given by Eq. 4.2.

$$f_L = \frac{7.2}{(L+r+p)\times k}\ GHz \tag{4.2}$$

where L = $\sqrt{3}H$, r = $\frac{3H}{4\pi}$ and 'H' is side length of hexagon.

For commonly used FR4 substrate with $\in_r$ = 4.4 and *h* = 0.159 cm, the empirical value of *k* = 1.15, determines lower band-edge frequency within 10% [47]. For presented design, Eq. 4.1 validates the value of lower band-edge frequency which is 2.75GHz in comparison to simulated and measured lower band-edge frequency of 2.64GHz, an error of 4%. The gain of the antenna is found to be 2-5dBi in the whole band of operation having maximum gain of 5.2dBi at 6.5GHz as shown in Fig. 4.12.

4.5 Summary

A novel hexagonal shaped monopole fractal antenna for UWB application is designed and presented in this chapter. As the second-iteration is used, the proposed antenna exhibits broad impedance bandwidth (-10 dB) covering a wide operating band (2.64GHz-6.96GHz), while maintaining the good radiation characteristics. The fabrication is done and the measured results validate the simulated characteristics. The variation with ground slot and ground slit are also simulated. It is observed that the impedance bandwidth drastically affected by ground slot. A band notch can also be created at desired frequency by using ground slit, which is tunable with the length of the slit, so that interference can be minimized in the desired band.

CHAPTER 5

NARROWBAND ANTENNA DESIGN

NARROWBAND ANTENNA DESIGN

This chapter presents novel, small and compact planar antennas having hexagonal patch with different fractal geometry in the ground plane. It has been found that modifying the ground plane using fractals on hexagonal patch results in lowering of resonant frequency by 55% in Antenna1 and improvement in impedance matching in Antenna2.Full ground plane is reformed by removing hexagonal carpet in Antenna1 and etching out Symmetrical Vertical Pyramidal Structure (SVPS) in Antenna2. Antenna1 is optimized for dual band operation and achieves satisfactorily 10dB impedance bandwidth at 3.176GHz and 4.552GHz while Antenna2 is having single band characteristic and resonate at 3.06GHz. Antnenna1 and Antenna2 are having gain around 5dBi (at both bands) and 3.3dBi respectively. Performance of the presented antennas is studied in terms of reflection coefficient (S11), radiation patterns, and gain. The presented antennas show a broadside radiation pattern in agreement with the conventional patch antennas. Both the presented geometry is fed by 50-ohm microstrip line. They are simulated using EM Simulation Software, tested and verified by measurement results. The measured results are well matched to the simulated output.

5.1 Introduction

The dramatic developments of a variety of wireless applications have remarkably increased the demand of multiband/wideband antennas with smaller dimensions than conventionally possible. Modern mobile devices need low-profile antennas [48]. The fact that different wireless standards, such as UMTS, WLAN and WiMAX, use different operation bands push the need for terminal antennas that are multiband and/or wideband [49]-[50]. The antennas should also be compatible in terms of cost, size, radiation patterns, gain and ease of integration in the printed circuit boards of communication devices. A number of antennas have been suggested [51]–[53], often with sizes that may be too large to be used practically.

Some compact antennas [54]–[56], have also been proposed. There is an important relation between antenna dimensions and wavelength. According to this relation, if antenna size is less than $\lambda/2$, then it is not an efficient radiator because radiation resistance, gain and bandwidth are reduced. So as size of antenna reduces, mismatch between antenna and source increases. Fractal geometry is a very good solution for this problem.

A fractal is a self-repetitive curve whose different parts are scaled copies of the whole geometry. Consequently, a radiator based on a fractal or self-similar geometry is expected to operate similarly at multiple wavelengths [57]-[58]-[25] and might keep similar radiation parameters through several bands. A multiband operation, in the 1-10GHz frequency range, was attained in [58] through the use of the Sierpinski gasket fractal. Key benefits of using fractal are reduced size and compactness. Fractals have space-filling property which leads to curves that are electrically very long, but fit into compact physical space. This property leads to the miniaturization of antenna elements. There are a variety of fractal shapes, such as Hilbert Curve [29], Sierpinski-carpet [45], Minkowski [21], Koch curve [19] etc. Lowering of resonant frequency and size reduction by using Sierpinski carpet is discussed in [59] where frequency has been lowered by almost 19% by etching out carpet from the radiating patch.

In this chapter two new hexagonal patch antennas are presented. The ground plane of Antenna1 is modified by etching out carpet fractal geometry which results in reduction of resonant frequency by 55% and it is finally optimized for dual band characteristics. In Antenna2, SVPS is introduced and removed from ground plane which maximizes the impedance matching and finally optimized for single band operation. In the following section, we discussed about the antennas geometries and the effects of modified ground plane. The simulated and measured radiation characteristics with peak gain of the antennas are also discussed. Finally conclusion is done in last section.

5.2 Design Parameters and Simulation Results

In this section the design consideration and corresponding results of both the antennas are explained one by one.

5.2.1 Antenna1: Design Parameters

The presented antenna consists of a 50-ohm micro-strip line fed hexagonal patch element mounted on a dielectric layer over a ground plane. This novel antenna has compact size of $50\times50mm^2$ including substrate.The low cost fiberglass dielectric substrate FR-4 is used having 1.6 mm of height and a relative permittivity of 4.4.The radiating element is hexagon of 15mm side length. In the beginning, patch with full ground plane is studied. Later a carpet of hexagons is etched out from the ground plane. The dimension of hexagons in the carpet is obtained by down-scaling the hexagonal patch to half of the whole dimension.

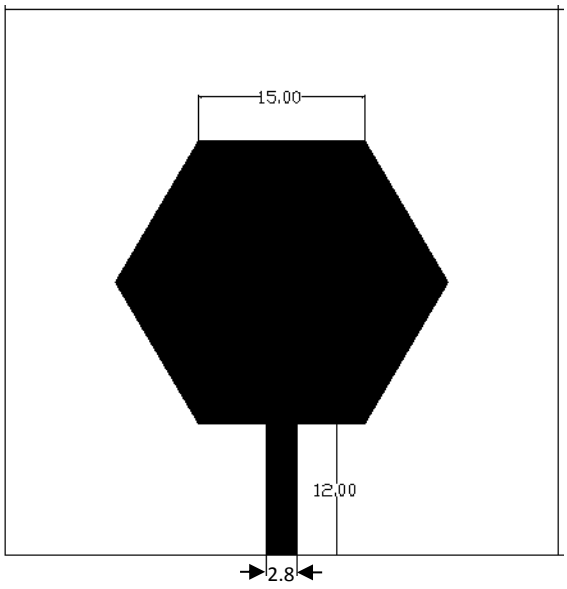

Figure 5.1 Geometry of the radiating element of Antenna1

The central element of the carpet is concentric with the patch while other elements are placed around its edges forming hexagonal carpet geometry. The surrounding elements are placed at a gap (*x*) from the central element as shown in Fig.5.2. Parametric study for *x* has been done. The final geometry is obtained and tested as shown in Fig.5.3.

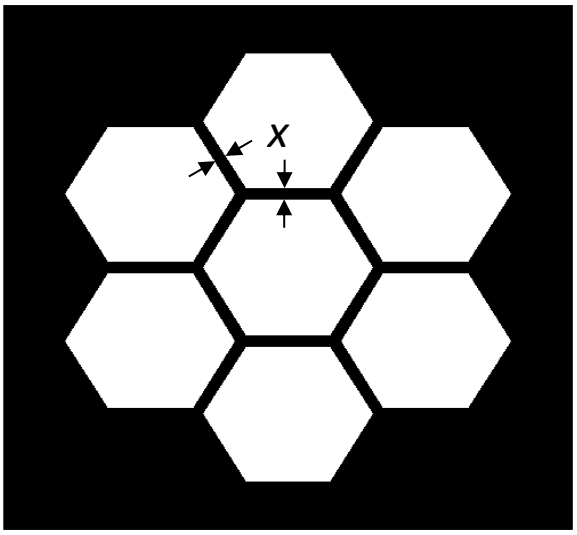

Figure 5.2 The ground plane with removed hexagonal carpet

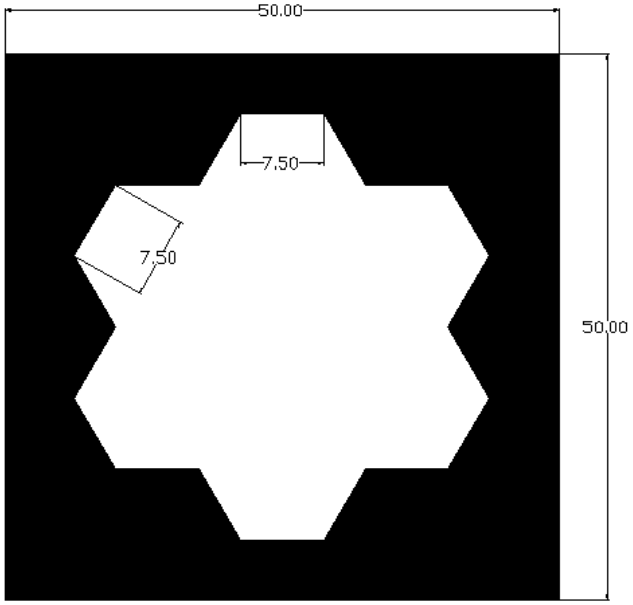

Figure 5.3 The ground plane (at *x*=0) of dual band antenna

5.2.2 Antenna1: Simulation Results

Antenna1 was simulated and optimized by using full wave EM simulation software. The simulated return loss against frequency for the presented antenna is shown in Fig. 5.4. Initially a conventional hexagonal patch with full ground plane is studied and it was found resonating at 5.8GHz. Later it has been observed that removing carpet of hexagonal elements from the full ground plane by keeping the surrounding element at a gap of *x*=3, the antenna

resonates at 2.632GHz i.e. a reduction of 55% in resonating frequency is achieved by using carpet fractal in ground plane.

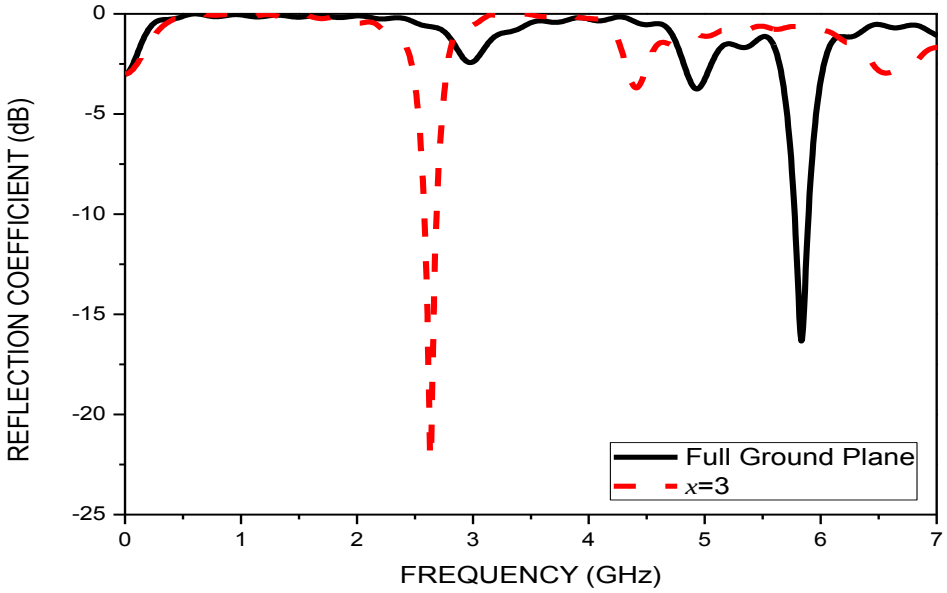

Figure 5.4 Return loss variation with full and modified ground plane

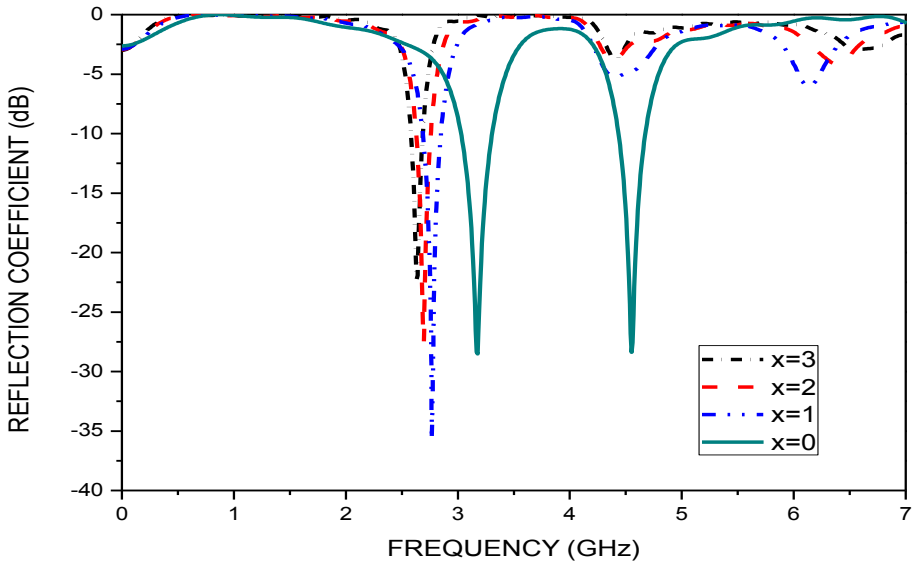

Figure 5.5 Return loss variation with gap(x)

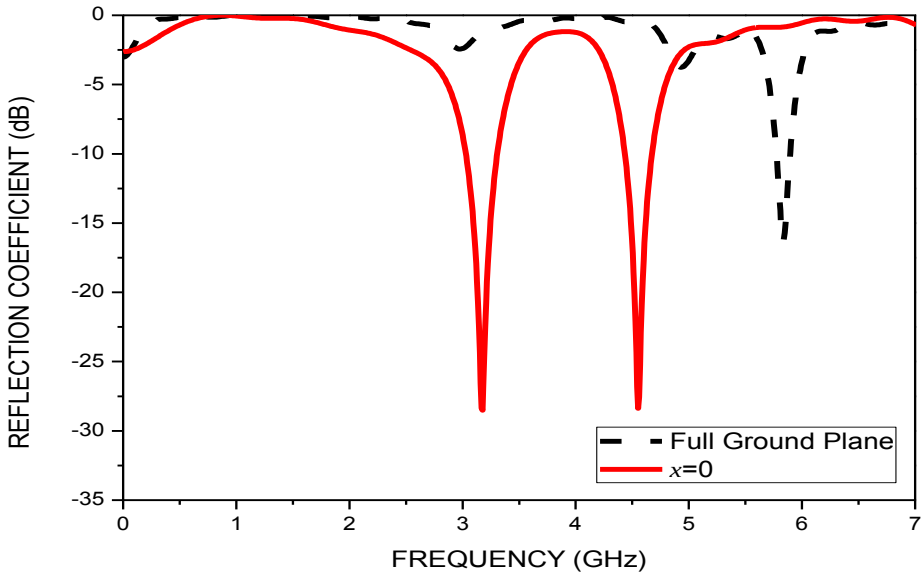

Figure 5.6 Return loss of final antenna at x=0

Table 5.1: Antenna1 Characteristics

Frequency (GHz)	3.176	4.552
Return loss (dB)	-28.51	-28.38
Bandwidth (%)	8.7	5.3
Gain (dBi)	4.88	5.71
Directivity (dBi)	5.08	6.41

Further, the resonance frequency vs. gap (x) is simulated and shown in Fig. 5.5, and found that the resonating frequency is slightly increasing with falling x and a new resonating band is observed for x=0, depicting a dual band characteristic. The antenna is optimized for a dual band operation. This dual band antenna delivers a return loss better than 25dB and gain of 4.88dBi and 5.71dBi at 3.176GHz and 4.552GHz, respectively. Table 5.1 summarizes the key parameters of the proposed dual band antenna.

5.2.3 Antenna2: Design Parameters

Antenna2 is even smaller than Antenna1 and it has total dimension of only 30x30mm^2 including substrate. It also consists of hexagonal radiating element but of smaller side length

of 8mm. Firstly, full ground plane is taken and studied. Then ground plane is modified by introducing and etching out Symmetrical Vertical Pyramidal Structure (SVPS). SVPS is obtained by taking two symmetrical horizontal rectangular geometries of 28mm length and 1mm width at the centre maintaining a gap of 1mm between them. Then the symmetrical geometries were scaled along length by 0.75 keeping width length constant.

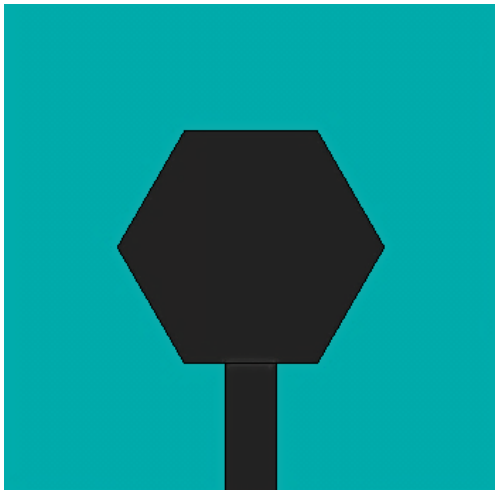

Figure 5.7 Geometry of radiating patch of Antenna2

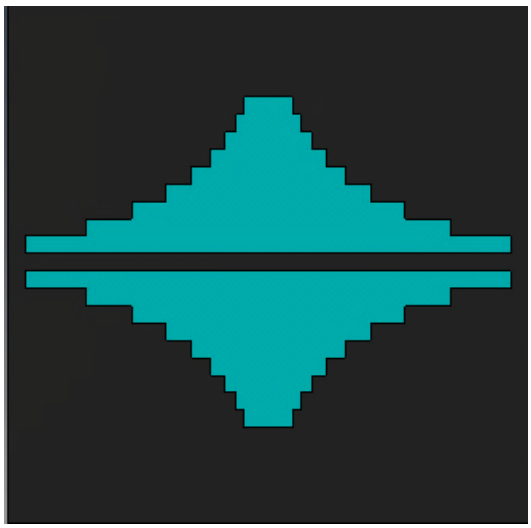

Figure 5.8 Ground plane geometry of Antenna2

The scaled parts were added to both, at the centre, of the previous parts already present and this process is iterated eight times to obtain final SVPS. For this design too, low cost and readily available FR4 substrate of relative permittivity of 4.4 and height 1.6mm has been used

and fed with 50-ohm microstrip line. Antenna2 patch geometry and ground plane geometry are shown in Figs.5.7 & 5.8.

5.2.4 Antenna2: Simulation Results

Antenna2 is simulated using EM Simulation Software. Initially antenna is simulated with full ground plane.

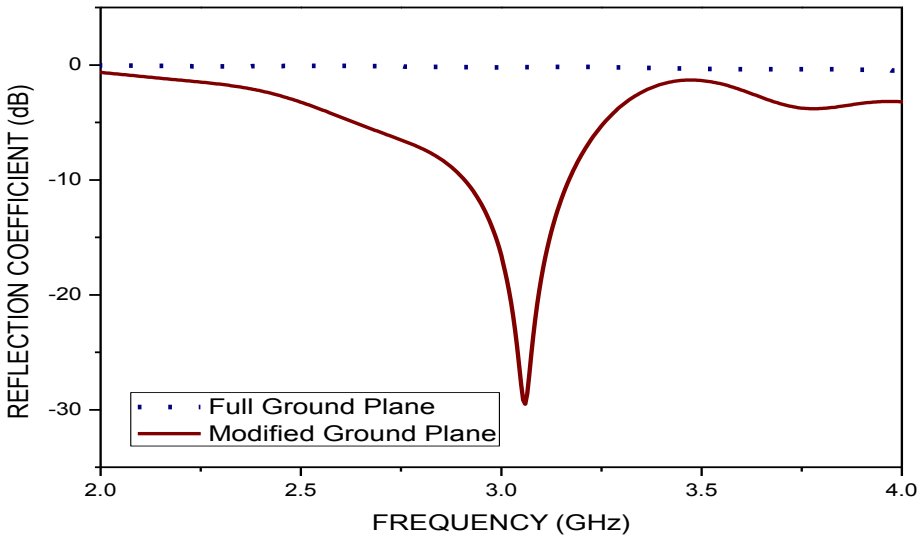

Figure 5.9 Return loss variation with full and modified ground plane

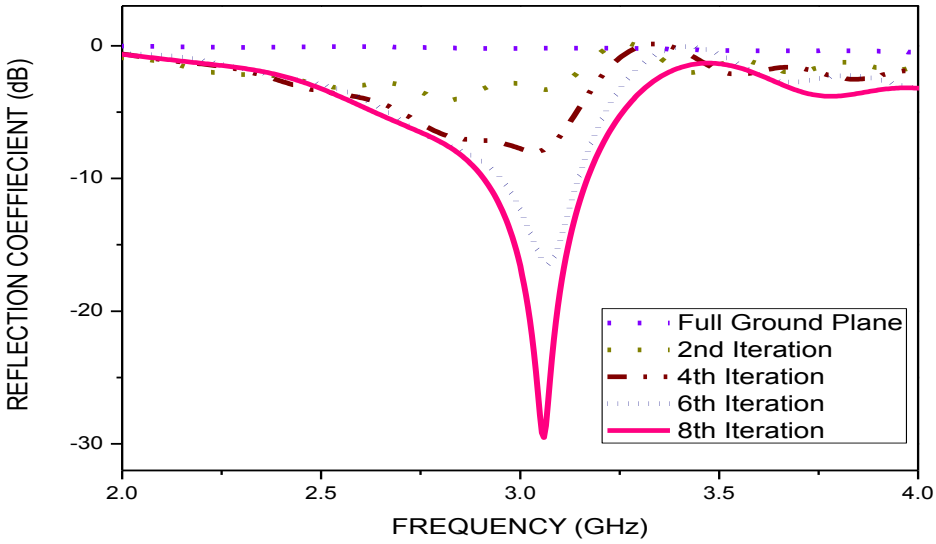

Figure 5.10 Return loss variation with iteration in ground plane

Then the effect of removing rectangular structure is observed. It is done till we reach final SVPS. The simulated results are shown in Figs. 5.9 & 5.10. Fig.5.9 shows the effect of even number iteration done in the ground plane as we ignore to show the results of odd iterations to present more clear results.

The simulated results show as we go on removing the rectangular structure, matching goes on increasing and antenna has a good performance with 10dB-return loss in the frequency range 2.9-3.17GHz that results in a fractional bandwidth (FBW) of 8.82%. Fig.5.10 depicts the comparison between full and final modified ground plane. It gives a clear view that matching has been improved too much at the desired frequency band by removing SVPS from the ground plane in comparison to full ground plane. The gain of the presented antenna is nearly 3.3dB.

5.3 Measured Results

In this section the antenna tested results are shown which is helpful to validate the simulated results.

5.3.1 Return Loss

In order to show the improved performance of the antennas with the modified ground plane, simulated results are compared through measurements in this section. Antennas are fabricated and tested in the Anechoic Chamber. Fabricated Antenna1 is shown in Fig.5.11. Fig.5.12 shows the measured vs. simulated plot for Antenna1. It shows that measured result is nearly matching with the simulated one. The simulated resonant frequency was at 3.176 GHZ & 4.552GHz and the measured resonant bands are found at 2.918GHz & 4.46GHz respectively. This slight variation occurs due to the uncertainty of the relative permittivity of our low-cost FR4 substrate for high frequencies.

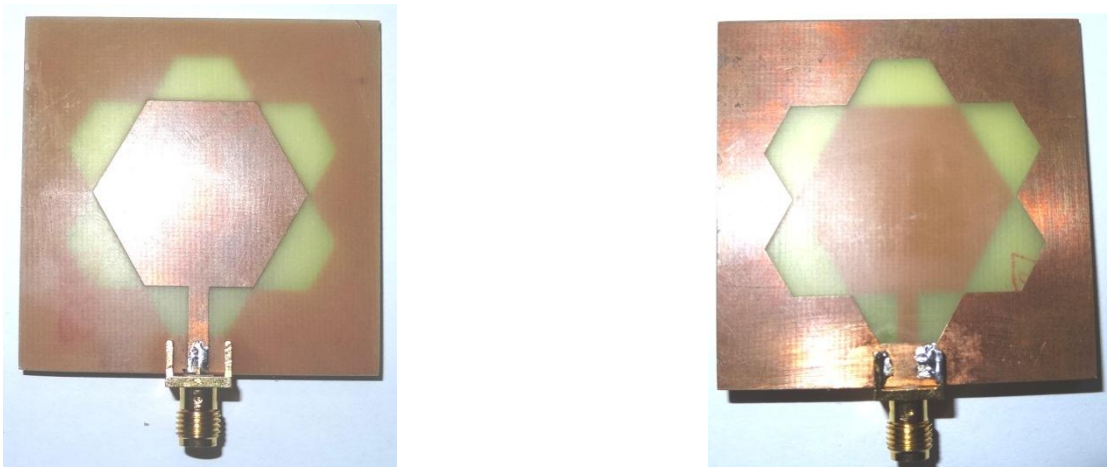

(a) (b)

Figure 5.11 Fabricated Antenna1 (a) Radiating Patch (b) Ground Plane

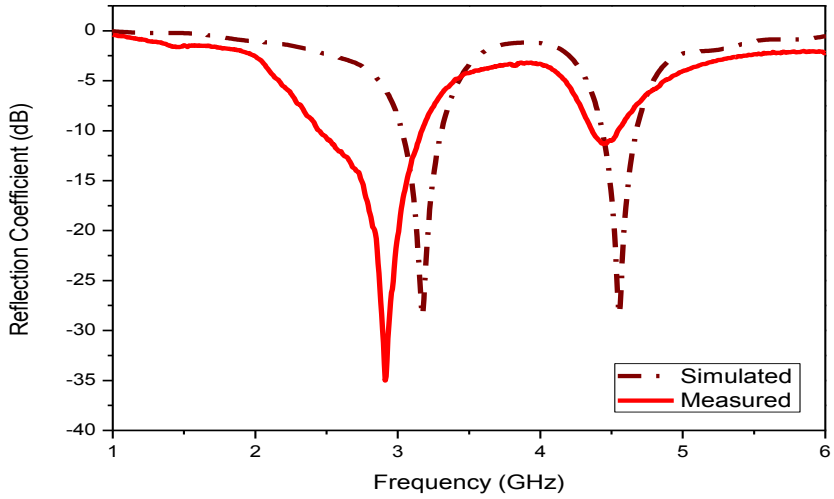

Figure 5.12 Measured vs Simulated Return loss of Antenna1

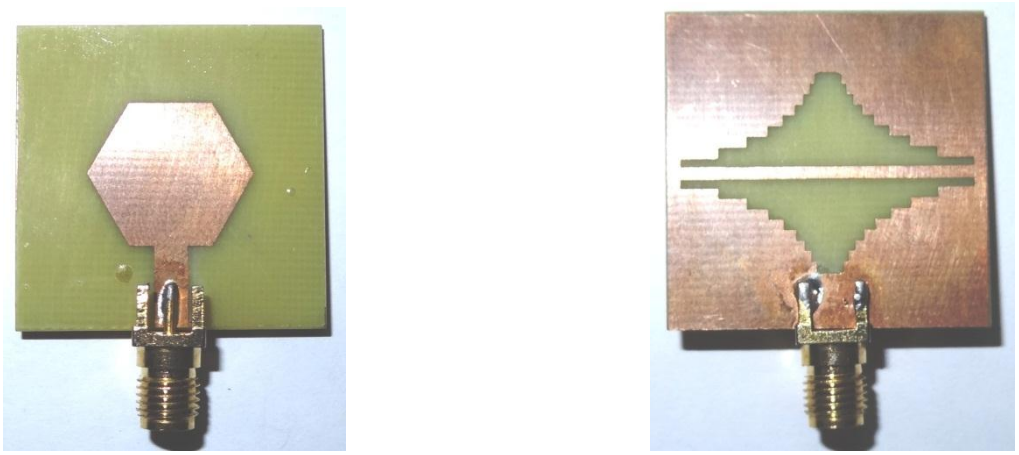

(a) (b)

Figure 5.13 Fabricated Antenna2 (a) Radiating Patch (b) Ground Plane

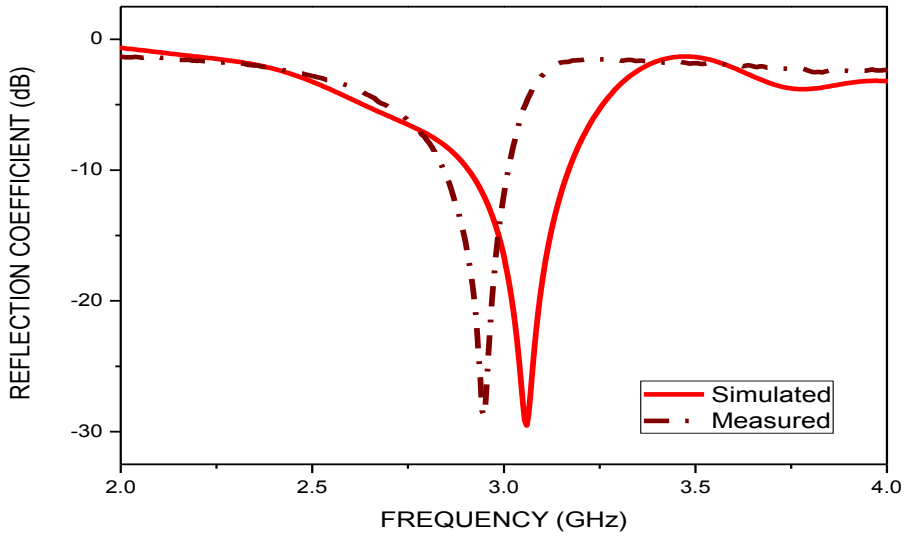

Figure 5.14 Measured vs Simulated Return loss of Antenna2

Similarly, Fabricated Antenna2 is shown in Fig.5.13. Fig. 5.14 describes the simulated vs. measured plot of Antenna2. In this plot too, measured plot is nearly matching with the simulated result. Simulation results show Antenna1 is resonating at 3.06GHz whereas it is resonating at 2.95GHz on measurement. The small frequency drift is produced by the error in the manufacturing and measurement.

5.3.2 Radiation Patterns

The radiation patterns of the antennas are measured in an anechoic chamber at 2.9185GHz and 4.46GHz for Antenna1 and at 2.95GHz for Antenna2 in the principal cuts. At each frequency, the radiation patterns in the E- and H-planes are normalized. Fig. 5.13(a) & (b) presents the co-polarisation and cross polarisation of Antenna1 at 2.9185GHz and 4.46GHz respectively and it is found that there a gap of around 15dBi between co and cross polarisation at both the bands making it a useful device for S & C-band applications having gain around 5dBi at both bands.

Fig. 5.13(c) shows co-polarisation and cross polarisation of Antenna2 at 2.95GHz. There is difference of approx. 20dBi between co and cross polarisation which make it an excellent gadget for S-band application having a gain of 3.3dBi.

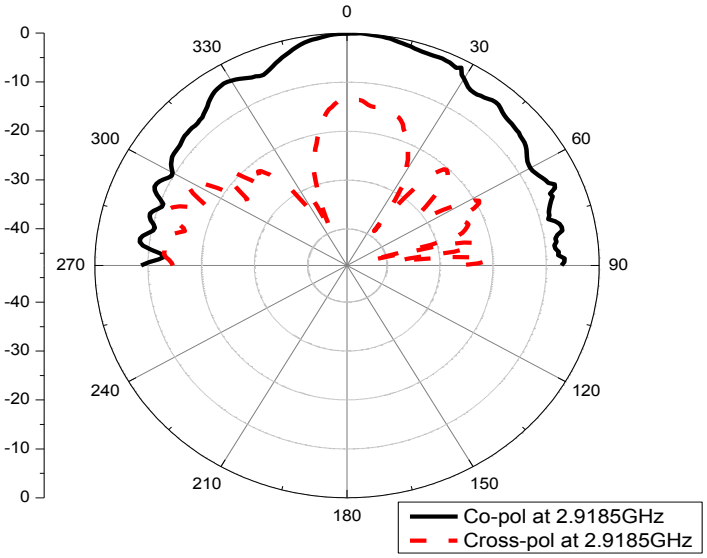
0
30
60
90
120
150
180
210
240
270
300
330
0
-10
-20
-30
-40
-40
-30
-20
-10
0
Co-pol at 2.9185GHz
Cross-pol at 2.9185GHz

(a)

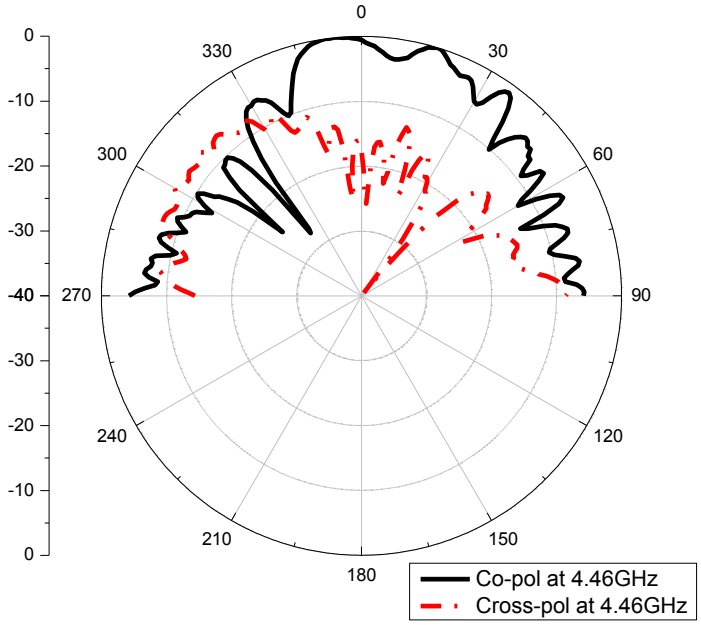
0
30
60
90
120
150
180
210
240
270
300
330
0
-10
-20
-30
-40
-30
-20
-10
0
Co-pol at 4.46GHz
Cross-pol at 4.46GHz

(b)

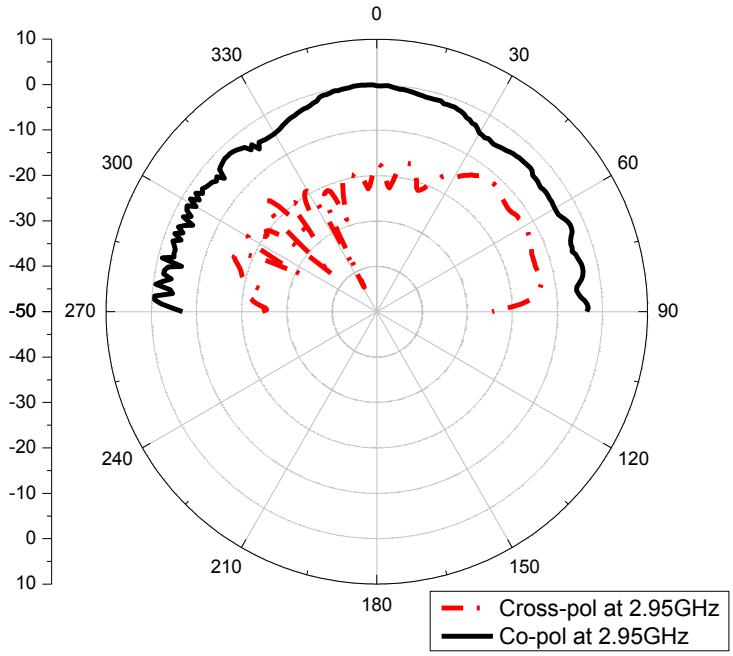

(c)

Figure 5.13 Measured Normalised Radiation patterns of antennas, (a) & (b) for Antenna1 and (c) for Antenna2, copolarization (continuous line), cross-polarization (dash line)

5.4 Summary

Two novel and compact hexagonal shaped patch with modified ground plane antenna are designed and presented. Antenna1 has carpet fractal geometry which is introduced to lower the resonant frequency. The resonance frequency of a conventional hexagonal patch with full ground is lowered by almost 55% by removing carpet of hexagonal elements from the full ground plane while maintaining the good radiation characteristics. A dual band characteristic is obtained by optimizing the gap (x). This antenna is optimized for S & C-band operation having a decent gain at both the bands. Antenna2 has SVPS removed from ground plane which improves the matching. It is optimized for S-band operation. It is having good gain of 3.3dBi at resonating point. The presented antennas show a broadside radiation pattern in agreement with the conventional patch antennas. The measurement results are also shown and found to be well matched to the simulated results.

CHAPTER 6

CONCLUSIONS AND FUTURE WORK

CONCLUSIONS AND FUTURE WORK

This chapter sums up the results and highlights the achievements of the research work carried out. This is followed by few suggestions for future work. The results presented in the thesis have been published by the author in different international journals and conferences.

6.1 Conclusions

In this work, fractal geometries are designed and implemented. For this, three antennas are designed using fractals. In fractal antennas, the self-similarity and plane-filling nature of fractal geometries are linked to its frequency characteristics. Fractals are geometrical shapes, which are self-similar, repeating themselves at different scales. Using fractal in an antenna maximizes the length, or increase the perimeter of material that can receive or transmit electromagnetic radiation within a given total surface area or volume.

Each design has specific characteristics and operates at different bands. The conclusions are as follows:

a) Both the characteristics i.e. Wideband and Multiband behavior of the antenna using fractals in hexagonal geometry have been successfully achieved.
b) Significant improvement in bandwidth is achieved by creating iterated fractal hexagons to increase the total perimeter (electrical length) of patch antenna to have wideband behaviour.
c) Fractional bandwidth greater than 90% is achieved for wideband antenna.
d) A controlled band notch is created in wideband characteristics to avoid interference at desired frequency.
e) With modification in the ground plane, narrowband characteristics have been successfully achieved with reduced dimension.

f) Reduction by almost 55% in resonant frequency is achieved by removing hexagonal carpet from the ground plane.

g) Modifying ground plane by etching out Symmetrical Vertical Pyramidal Structure (SVPS) helps to design an smaller antenna for S-band application.

h) The theoretical and simulated different characteristics of antennas such as return loss, radiation pattern, gain, etc. are verified by measuring those antennas.

i) All measured results are found well matched to simulated results.

All the presented designs are simulated using CST Microwave Studio Suite12. Designs are made using FR4 substrate having ε_r value 4.4 and height of 1.6mm which is a low cost material and easily available in the market. Microstrip feed line of 50Ω is used in every case. Measurement of all the antennas is done using the lab facility of ISAC-Bangalore. The small frequency drift seen in measurement results is produced by the error in the manufacturing and measurement.

6.2 Suggestions for Future Work

The following are some of the prospects for future work:

a) The whole band of UWB (i.e. 3.2GHz - 10.6GHz) is not covered in wideband antenna. New techniques can be employed in future to increase the matching i.e. fractional bandwidth of antenna.

b) The gain of the narrow band antennas designed is low, so in future other techniques can be employed to increase the gain of these antennas.

c) FEM can be employed to solve and implement all the designs.

Publications

International Conferences

[1] **Sonu Agrawal,** R. D. Gupta and S. K. Behera, "A New Dual Band Antenna with Hexagonal Carpet in Ground Plane," 8th International Conference on Microwaves, Antenna Propagation and Remote Sensing (ICMARS), Jodhpur, Rajasthan, India, pp. 415-418, Dec 2012.

[2] **Sonu Agrawal,** R. D. Gupta and S. K. Behera, "A Hexagonal Shaped Fractal Antenna for UWB Application", IEEE 2012 International Conference on Communications, Devices and Intelligent Systems (CODIS), ISBN 978-1-4673-4700-6/12, Kolkata, India, pp. 535-538, Dec 2012.

National Conference

[1] R. D. Gupta, **Sonu Agrawal** and S. K. Behera, "Design of a Compact Reconfigurable RDRA," 19th National Conference on Communication (NCC), 978-1-4673-5952-8/13, IIT Delhi, India, Feb 2013.

International Journals

[1] **Sonu Agrawal** and S. K. Behera, "On Design of Different Fractal Ground Geometries on Hexagonal Patch Antenna," International Journal of RF and Microwave Computer-Aided Engineering, Wiley (Communicated)

[2] **Sonu Agrawal**, R. D. Gupta and S. K. Behera, "Design of Wideband Planar Hexagonal Fractal Antenna Having Notch-Band Characteristics," Journal of Electromagnetic Waves and Applications, Taylor & Francis. (Communicated)

References

[1] J. G. Proakis, Digital Communications, New York: McGraw-Hill, 1989.

[2] C. E. Shannon, “A Mathematical Theory of Communication", Bell Syst. Tech. J., vol. 27, July & October 1948, pp. 379-423, 623-656.

[3] FCC 802 Standards Notes, “FCC first report and order on ultra-wideband technology,” 2002.

[4] Zhi Ning Chen and Michael Y. W. Chia, “Broadband Planar Antennas, Design and Applications,” John Wiley & Sons, Ltd.

[5] E. E. C. de Oliveira, P. H. da F. Silva, A. L. P. S. Campos, S. Gonc, A.D.Silva, “Overall Size Antenna Reduction using Fractal Geometry”, *Microwave and Optical Technology Letters,* vol. 51, no. 3, March 2009, pp. 671 -674.

[6] G. A. Deschamps, “Microstrip Microwave Antennas,” *3rd USAF Symposium on Antennas,* 1953.

[7] H. Gutton and G. Baissinot, “Flat Aerial for Ultra High Frequencies,” French Patent no. 703 113, 1955.

[8] C. A. Balanis, “Antenna Theory - Analysis and Design,” 2nd edition, John Wiley.

[9] Kin-Lu Wong, “Planar Antennas for Wireless Communications,” *Wiley,* December, 2002.

[10] P. Bhartia, I. Bahl, R. Garg, and A. Ittipiboon, *Microstrip Antenna Design Handbook*, Artech House.

[11] Lee, K. F., Chen, W., *Advances in Microstrip and Printed Antennas,* Wiley, 1997.

[12] D. M. Pozar, “Microstrip Antennas,” *Proc. IEEE,* vol. 80, no. 1, January 1992, pp.79-81.

[13] D. M. Pozar and B. Kaufman, "Increasing the Bandwidth of the Microstrip Antenna by Proximity Coupling," *Electronics Letters*, vol. 23, no. 8, April 1987.

[14] K. R Carver and J. W Mink, "Microstrip Antenna Technology," *IEEE Trans. Antennas Propagate.*, vol. AP-29, no. 1, January 1981, pp. 2-24.

[15] M. N. O. Sadiku, "A Simple Introduction to Finite Element Analysis of Electromagnetic Problems," *IEEE Trans. Educ.*, vol. 32, no. 2, May 1989, pp. 85-93.

[16] M.N.O. Sadiku, *Numerical Techniques in Electromagnetics,* CRC Press, 2nd ed., 2001.

[17] P. P. Silvester and R. L. Ferrari, *Finite Elements for Electrical Engineers,* Cambridge: Cambridge University Press, 3rd ed., 1996.

[18] B. B. Mandelbrot, "The fractal Geometry of Nature," New York: W. H. Freeman, 1983.

[19] M. N. A. Karim, M. K. A. Rahim, T. Masri, "Fractal Koch Dipole Antenna for UHF Band Application", Microwave and Optical Technology Letters, Vol. 51, No. 11, November 2009, pp. 2612-2614.

[20] Ramadan, A., K. Y. Kabalan, A. El-Hajj, S. Khoury, and M. Al-Husseini, "A reconfigurable U-koch microstrip antenna for wireless applications," *Progress In Electromagnetics Research*, PIER 93, 2009, pp. 355-367.

[21] S. Suganthi, S. Raghavan, "Design and Simulation of Planar Minkowski Fractal Antennas", *Wireless Communication, Vehicular Technology, Information Theory and Aerospace & Electronic Systems Technology* (Wireless VITAE), 2011.

[22] J. P. Gianvittorio and Y. Rahmat-Sami "Fractal Antennas: A Novel Miniaturization Technique and Applications," *IEEE Antennas Propagation Mag.*, vol. 44, no.1, 2002, pp. 20-36.

[23] D. H. Werner and S. Ganguly, "An Overview of Fractal Antenna Engineering Research," *IEEE Antennas and Propagation*, vol. 45, no. 1, February 2003, pp. 38-57.

[24] C.Puente, Romeu, et al., “Fractal Multi-band Antenna Based on the Sierpinski Gasket,” *Electronics Letters,* vol. 32, no. 1, January 1996, pp. 1-2.

[25] D.A Sanchez-Hernandez, "Multiband Integrated Antennas for 4G Terminals,” Artech House, inc, Norwood, 2008, pp. 95-102.

[26] S. Best, “The fractal loop antenna: a comparison of fractal and non-fractal geometries,” *IEEE, Antennas and Propagation Society International Symposium*, vol. 3, 2001, pp. 146-149.

[27] Y. Li, X. Yang, C. Liu and T. Jiang, “Miniaturization Cantor Set Fractal Ultra-wideband Antenna with A Notch Band Characteristic,” *Microwave and Optical Technology Letters,* vol. 54, issue 5, May 2012, pp. 1227–1230.

[28] Y. Li, W. Li, C. Liu and T. Jiang, “Cantor Set Fractal Antennas for Switchable Ultra Wideband Communication Applications,” vol. 3, May 2012, pp. 1-4.

[29] J. C Liu, B. H. Zeng, H. L. Chen, S. S. Bor and D. C. Chang, “Compact Fractal Antenna with Self-Complimentary Hilbert Curves for WLAN Dual-band and Circular Polarization Applications,” *Microwave and Optical Technology Letters,* vol. 52, no. 11, November 2010, pp. 2535-2539.

[30] H. O. Peitgen, J. M. Henriques and L. F. Penedo, “Fractals in the Fundamental and Applied Sciences,” Amsterdam: North Holland, 1991.

[31] K. J. Vinoy, et al., “Resonant Frequency of Hilbert Curve Fractal Antennas,” *Proc. IEEE Antennas and Propagation Society Int. Symposium*, vol. 3, July 2001, pp. 648-651.

[32] J. Anguera, C. Puente and J. Soler, “Miniature Monopole Antenna Base on the Fractal Hilbert Curve,” *Proc. IEEE Antennas and Propagation Society Int. Symposium*, vol. 4, June 2002, pp. 546-549.

[33] P. S. Addison, “Fractal and Chaos: An illustrated Course,” Bristol, U.K: Institute of Physics Publishing, 1997.

[34] H. O. Pietgen, H. Jurgens and D. Saupe, “Chaos and Fractals: New Frontiers of Science,” New York: Springer-Verlag, 1992.

[35] E. E. C. de Oliveira, P. H. da F. Silva, A. L. P. S. Campos, S. Gonc and A. D. Silva, “Overall Size Antenna Reduction using Fractal Geometry,” *Microwave and Optical Technology Letters*, vol. 51, no. 3, March 2009, pp. 671-674.

[36] M. Naghshvarian-Jahromi and A. Falahati, “Classic miniature fractal monopole antenna for UWB applications,” presented at the ICTTA’08, Damascus, Syria, April 2008.

[37] M. Naghshvarian-Jahromi and N. Komjani, “Analysis of the behaviour of Sierpinski carpet monopole antenna,” *Appl. Comput. Electromagn. Society J., ACES*, to be published.

[38] C. T. P. Song, P. S. Hall, H. Ghafouri-Shiraz, and D. Wake, “Fractal stacked monopole with very wide bandwidth,” *Electron. Let.*, vol. 35, no. 12, , June 1999, pp. 945–946.

[39] C. Puente-Baliarda, J. Romeu, R. Pous, and A. Cardama, “On the behaviour of the Sierpinski multiband fractal antenna,” *IEEE Trans. Antennas Propag.*, vol. 46, 1998 pp. 517–524.

[40] M. Naghshvarian-Jahromi, “Novel miniature semi-circular-semifractal monopole dual band antenna,” *J. Electromagn. Wave Applicat., JEMWA*, vol. 22, 2008, pp. 195–205,.

[41] G. J. Walker and J. R. James, “Fractal volume antennas,” *Electron. Lett.*, vol. 34, no. 16, August 1998, pp. 1536–1537.

[42] J. Young and L. Peter, “A brief history of GPR fundamentals and applications,” in *Proc. 6th Int. Conf. Ground Penetrating Radar*, 1996, pp.5–14.

[43] D. J. Daniels, “Surface-Penetrating Radar,” *IEEE Radar Sonar Navigation Avionics Series 6*. New York: IEEE Press, 1996, pp. 72–93.

[44] J. C Liu, B. H. Zeng, H. L. Chen, S. S. Bor and D. C. Chang, “Compact Fractal Antenna with Self-Complimentary Hilbert Curves for WLAN Dual-band and Circular Polarization Applications”, *Microwave and Optical Technology Letters*, vol. 52, no. 11, November 2010, pp. 2535-2539.

[45] Y. K. Wang, J. S. Luo and Y. Li, “Investigations on the K-Sierpinski Carpet Fractal Antenna”, *2011 Cross Strait Quad-Regional Radio Science and Wireless Technology Conference*, July 2011, pp. 382-385.

[46] C.P. Baliarda, J.Romeu, A.Cardama, “The Koch Monopole: A Small Fractal Antenna”, *IEEE Transactions on Antennas and Propagation*, vol. 48, no. 11, November 2000, pp. 1773-1781.

[47] K. P. Ray, “Design Aspects of Printed Monopole Antennas for Ultra-Wide Band Applications,” *International Journal of Antennas and Propagation*, January 2008.

[48] K. L. Wong, Planar Antennas for Wireless Communications. Hoboken, NJ: Wiley, 2003.

[49] Torpi, H. and Y. Damgaci, “Design of dual-band reconfigurable smart antenna," *PIERS Proceedings*, 425-429, Prague, Czech Republic, August 27-30, 2007.

[50] Liu, W. C., W. R. Chen, and C. M. Wu, “Printed double S-shaped monopole antenna for wideband and multiband operation of wireless communications," *IEE Proc.-Microw. Antennas Propag.*, Vol. 151, No. 6, 473-476, December 2004.

[51] Y. L. Kuo and K. L. Wong, “Printed double-T monopole antenna for 2.4/5.2 GHz dual-band WLAN operations,” *IEEE Trans. Antennas Propag.*, vol. 51, no. 9, pp. 2187–2192, Sep. 2003.

[52] H. D. Chen, J. S. Chen, and Y. T. Cheng, “Modified inverted-L monopole antenna for 2.4/5 GHz dual-band operations,” *Electron. Lett.*, vol. 39, pp. 1567–1568, Oct. 2003.

[53] B. S. Yildirim, “Low-profile and planar antenna suitable for WLAN/ Bluetooth and UWB application,” *IEEE Antennas Wireless Propag.Lett.*, vol. 5, pp. 438–441, 2006.

[54] W. C. Liu, “Wideband dual-frequency double inverted-L CPW-fed monopole antenna for WLAN application,” *IEE Proc. Microw., Antennas Propag.*, vol. 152, pp. 505–510, 2005.

[55] T. H. Kim and D. C. Park, “Compact dual-band antenna with double L-slits for WLAN operations,” *IEEE Antennas Wireless Propag. Lett.*, vol. 4, pp. 249–252, 2005.

[56] J. Liang, C. C. Chiau, X. Chen, and C. G. Parini, “Study of a printed circular disc monopole antenna for UWB systems,” *IEEE Trans. Antennas Propag.*, vol. 53, no. 11, pp. 3500–3504, Nov. 2005.

[57] S. E. El-Kharny, "New Trends in Wireless Multimedia Communications based on Chaos and fractals," ‘zr’ National Radio Science Conference, March 16-18, 2004, pp 1-25.

[58] M. K. A. Rahim, M. Z. A. Abdul Aziz, N. Abdullah, "Wideband Sierpinski Carpet Monopole Antenna," Proceedings of Asia-Pacific Conference on Applied Electromagnetics, December 20-21, 2005, pp. 62-65, Malaysia.

[59] W. L. Chen and G. M. Wang, “Small Size Edge-Fed Sierpinski Carpet Microstrip Patch Antennas,” Progress In Electromagnetics Research C, Vol. 3, 2008.